

## Electronic Supplementary Information (ESI)

### Non-ionic self-assembling amphiphilic polyester dendrimers as new drug delivery excipients

Dhiraj R. Sikwal, Rahul S. Kalhapure\*, Mahantesh Jadhav, Sanjeev Rambharose, Chunderika Mocktar and Thirumala Govender\*

Discipline of Pharmaceutical Sciences, University of KwaZulu-Natal, Private Bag X54001 Durban, 4000, South Africa.

\*Corresponding Author: Private Bag X54001 Durban, 4000, KwaZulu-Natal, South Africa. Tel: 00 27 31 260 7358, Fax: 0027 31 260 7792. email: govenderth@ukzn.ac.za (T. Govender), kalhapure@ukzn.ac.za; rahul.kalhapure@rediffmail.com (R.S. Kalhapure).

#### 1. Experimental section- Supporting information

##### 1.1 In vitro cytotoxicity

The GMS and GMOA ADs were evaluated for their biocompatibility by in vitro cytotoxicity through a MTT assay.<sup>1</sup> Breast adenocarcinoma (MCF 7), human liver hepatocellular carcinoma (Hep G2) and human lung carcinoma (A549) cell lines were cultured in complete medium at 37 °C in humidified atmosphere of 5% in air. All cell lines harvested in the exponential phase were seeded equivalently ( $2.2 \times 10^3$ ) in a 96 well plate and allowed to adhere by incubating for 24 h. Thereafter, the culture media was replaced with 100  $\mu$ l fresh medium and sample stock solution in distilled water was added to the medium to achieve concentrations of 20, 40, 60, 80 and 100  $\mu$ g/ml. The wells containing only medium were considered as controls and wells with only media without cells were considered as blank. All experiments were performed in four replicates. After incubation for 48 h, the culture media with compounds were removed and replaced with 100  $\mu$ l fresh media and 100  $\mu$ l MTT solution (5 mg/ml in PBS) for each well and again incubated for 4 h. After 4 h of incubation,

the media and MTT solution were removed and replaced with 100  $\mu$ l of DMSO to solubilize MTT formazan. Optical density (OD) of each well was determined at wavelength of 540 nm using a microplate spectrophotometer (Spectrostar nano, Germany). Percentage cell viability was calculated using the following equation.

$$\% \text{ cell survival} = (A_{540 \text{ nm treated cell}} / A_{540 \text{ nm untreated cells}}) \times 100$$

### **1.2 HPLC method for determination of FSD<sup>2</sup>**

Reverse phase C18 column (Nucleosil 120-5 C18; 4 x 150 mm, 5  $\mu$ m) was used and the mobile phase was consists of a 3:1 mixture of methanol and 0.01 M Potassium hydrogen phosphate. The column temperature, flow rate, injection volume and detection wavelength were 25  $^{\circ}$ C, 2 ml/minute, 20  $\mu$ L and 254 nm respectively. The retention time (RT) for FSD was 7.1  $\pm$  0.19. The standard calibration curve was determined within concentration range of 5 to 30  $\mu$ g/ml.

### **1.3 Determination of %EE and percentage drug loading (%DL)**

The %EE of FSD loaded ADs micelles was determined as per reported centrifugal-ultrafiltration method.<sup>3</sup> Briefly 1 ml of FSD loaded ADs micelles were added into Amicon® Ultra-4, centrifugal filter tubes (MWCO10 kDa, Millipore Corp., USA) and centrifuged for 30 min at 5000 rpm. The amount of FSD in ultrafiltrate was determined by HPLC method as per previous section. The total amount of FSD was determined by dissolving FSD loaded ADs micelles in to methanol and HPLC analysis of it. %EE and %DL of FSD loaded micelles was determined by following equation.

$$\%EE = C_0 - C / C_0 \times 100$$

$$\%DL = C_0 - C / C_0 - C + C_m \times 100$$

Where C is the FSD concentration in ultrafiltrate, C<sub>0</sub> is the concentration of FSD in drug loaded micelles and C<sub>m</sub> is the concentration of ADs in the micelles.

## 2. Results section – Supporting information

**Table S1.** Elemental analysis of ADs.

AD	Observed values		Theoretical values	
	C [%]	H [%]	C [%]	H [%]
GMS-G2-OH	57.31	8.62	58.05	8.60
GMS-G3-OH	55.08	8.06	55.09	7.82
GMOA-G2-OH	55.88	8.64	58.16	8.42
GMOA-G3-OH	54.62	7.87	55.14	7.73

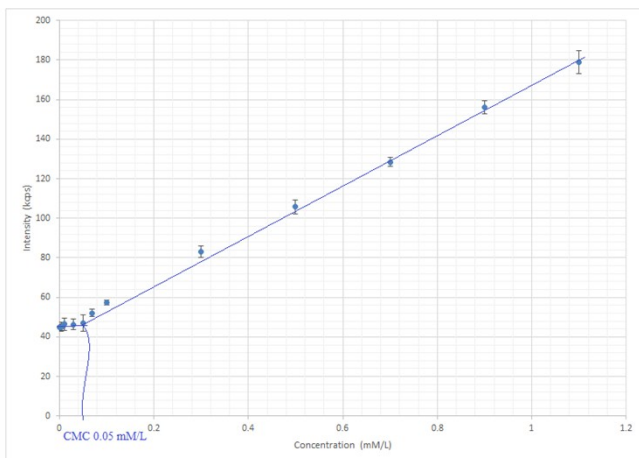
**Table S2.** Effect of FSD solubilization on size, PDI and ZP of aggregates of amphiphiles.

Formulations	Size (nm)	PDI	ZP (mV)
GMS-G2-OH	7.6 ± 0.13	0.26 ± 0.05	-2.61 ± 0.12
FSD-GMS-G2-OH	22.15 ± 3.5	0.75 ± 0.03	-16 ± 0.52
GMS-G3-OH	6.48 ± 0.04	0.62 ± 0.06	-0.01 ± 0.05
FSD-GMS-G3-OH	6.48 ± 0.71	0.20 ± 0.04	-12.6 ± 1.5
GMOA-G2-OH	8.62 ± 0.48	0.27 ± 0.03	-5.5 ± 0.76
FSD-GMOA-G2-OH	7.2 ± 0.09	0.34 ± 0.02	-15.5 ± 0.4
GMOA-G3-OH	12.38 ± 0.36	0.34 ± 0.02	-7.9 ± 0.763
FSD-GMOA-G3-OH	12.55 ± 1.18	0.35 ± 0.07	-7.9 ± 1.02
PF-68	28.67 ± 4.87	0.716 ± 0.02	-2.39 ± 0.40
FSD-PF-68	142.6 ± 9.86	0.625 ± 0.06	-2.91 ± 0.57

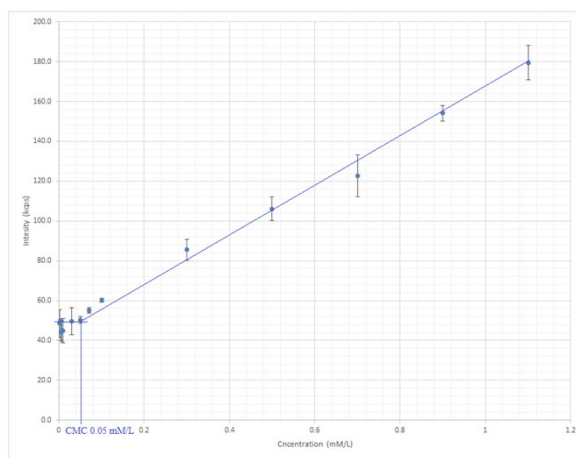
NA = Not applicable

**Table S3.** Amount of unentrapped, entrapped FSD and %EE of micelles from ADs

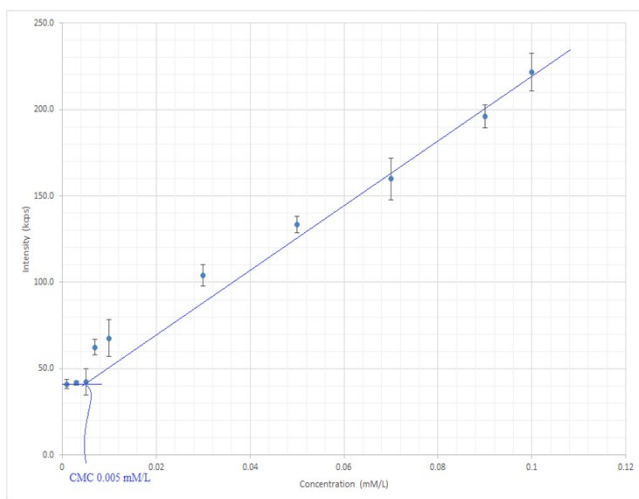
ADs	Total FSD content (µg/ml)	Unentrapped FSD (µg/ml)	Entrapped FSD (µg/ml)	%EE	%DL
GMS-G2-OH	29.0 ± 3.4	26.7 ± 0.5	2.3 ± 0.5	8.0 ± 1.9	0.023 ± 0.005
GMS-G3-OH	21.9 ± 1.7	20.9 ± 0.2	1.0 ± 0.2	4.5 ± 0.9	0.01 ± 0.002
GMOA-G2-OH	136.4 ± 3.27	101.3 ± 0.1	35.1 ± 0.1	25.76 ± 0.1	0.350 ± 0.001
GMOA-G3-OH	34.91 ± 0.83	30.6 ± 0.3	4.3 ± 0.3	12.3 ± 0.9	0.043 ± 0.003
PF-68	11.1 ± 0.1	10.4 ± 0.1	0.7 ± 0.1	6.6 ± 1.0	0.007 ± 0.001



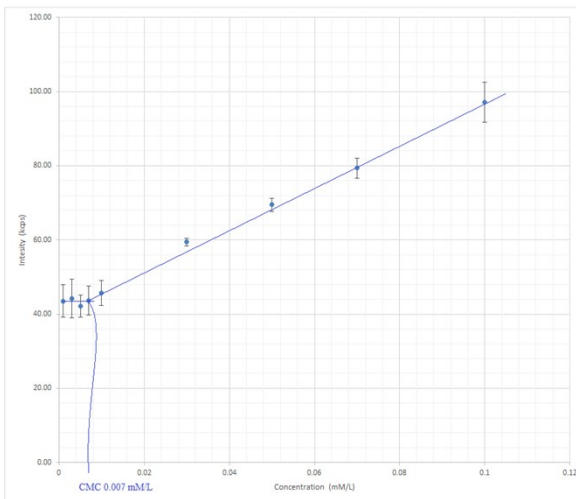
(A)



(B)



(C)



(D)

**Fig. S1.** CMC of (a) GMS-G2-OH, (B) GMOA-G2-OH, (C) GMS-G3-OH, (D) GMOA-G3-OH.

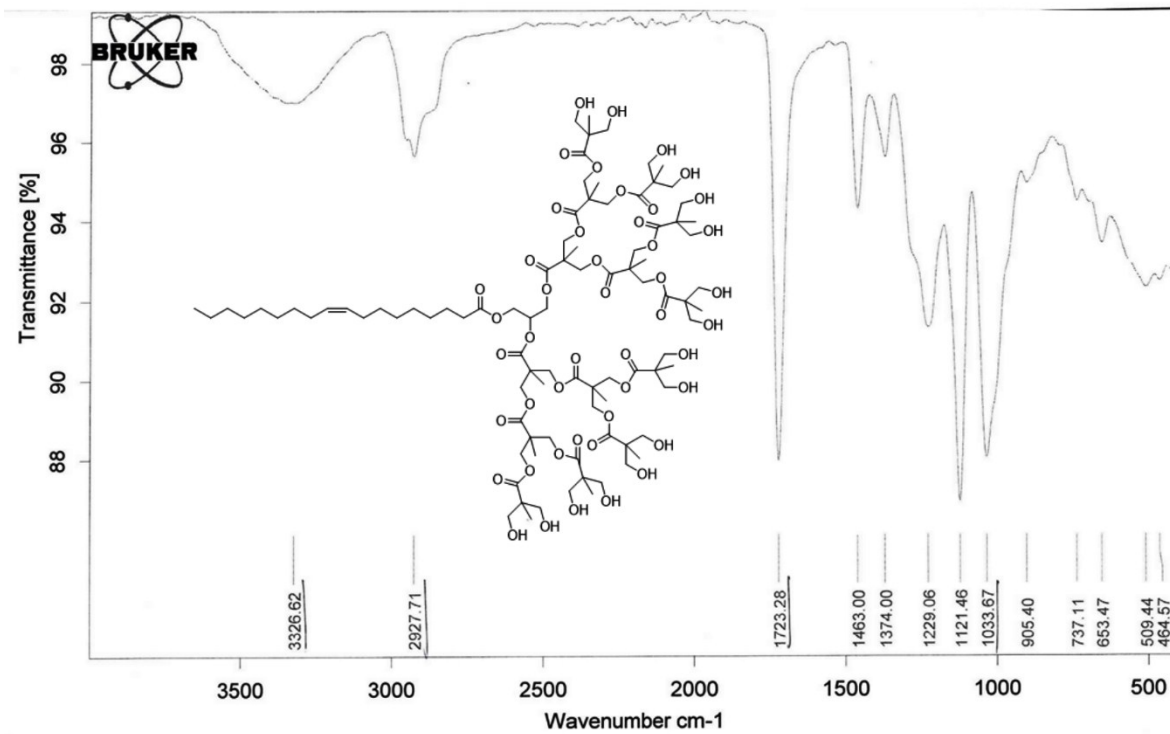
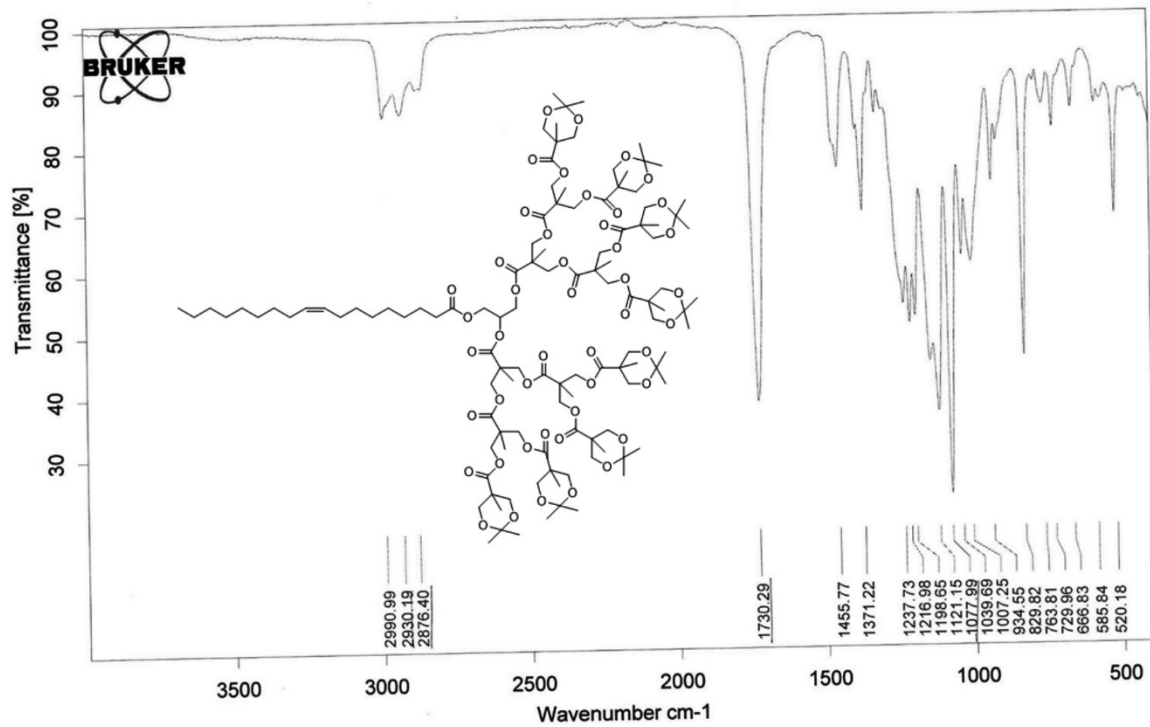
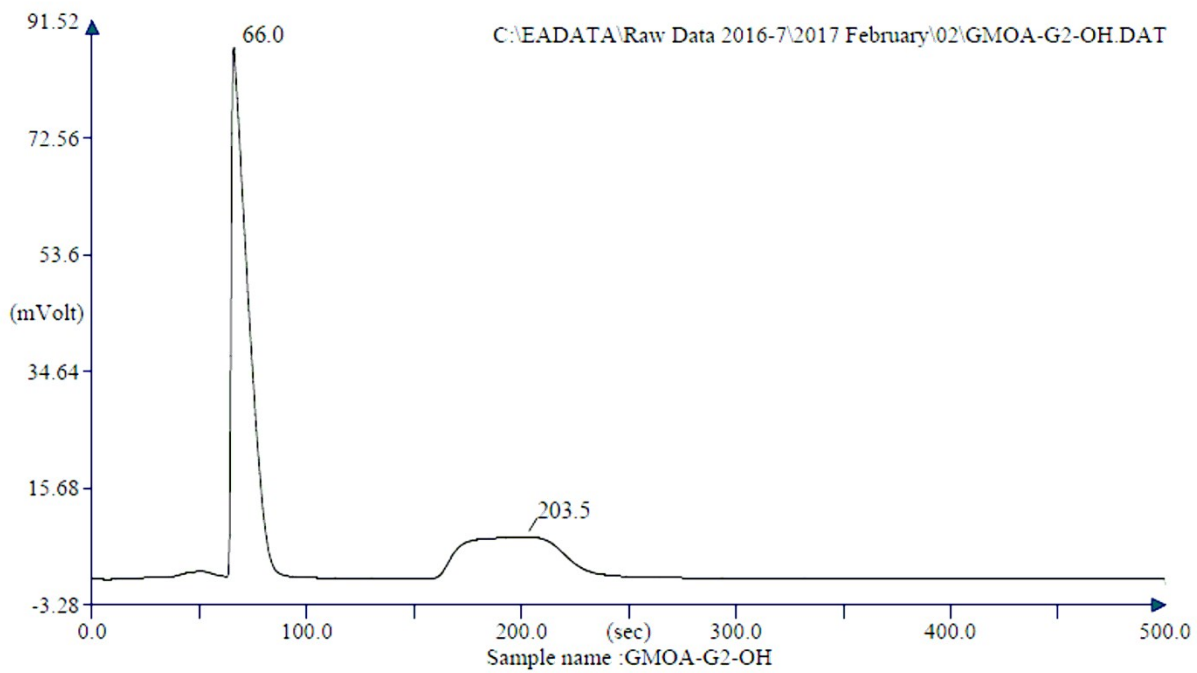
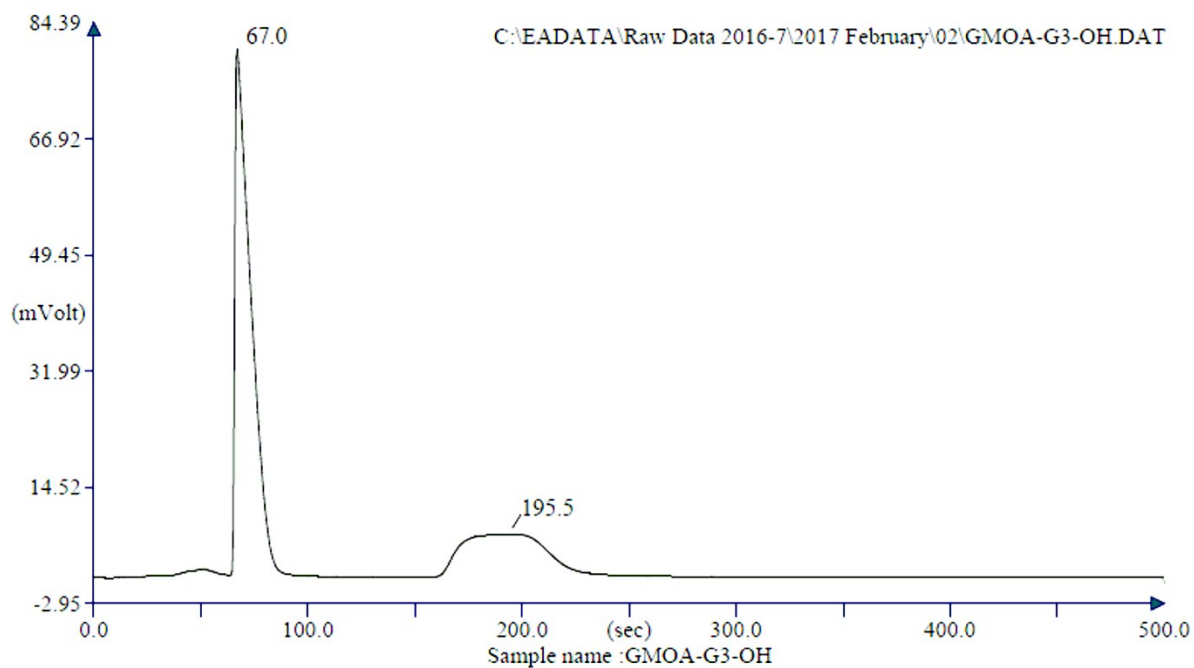


**Fig. S2.** Comparative FT-IR of GMOA-G3-Me and GMOA-G3-OH for confirmation of deprotection of acetonide group.



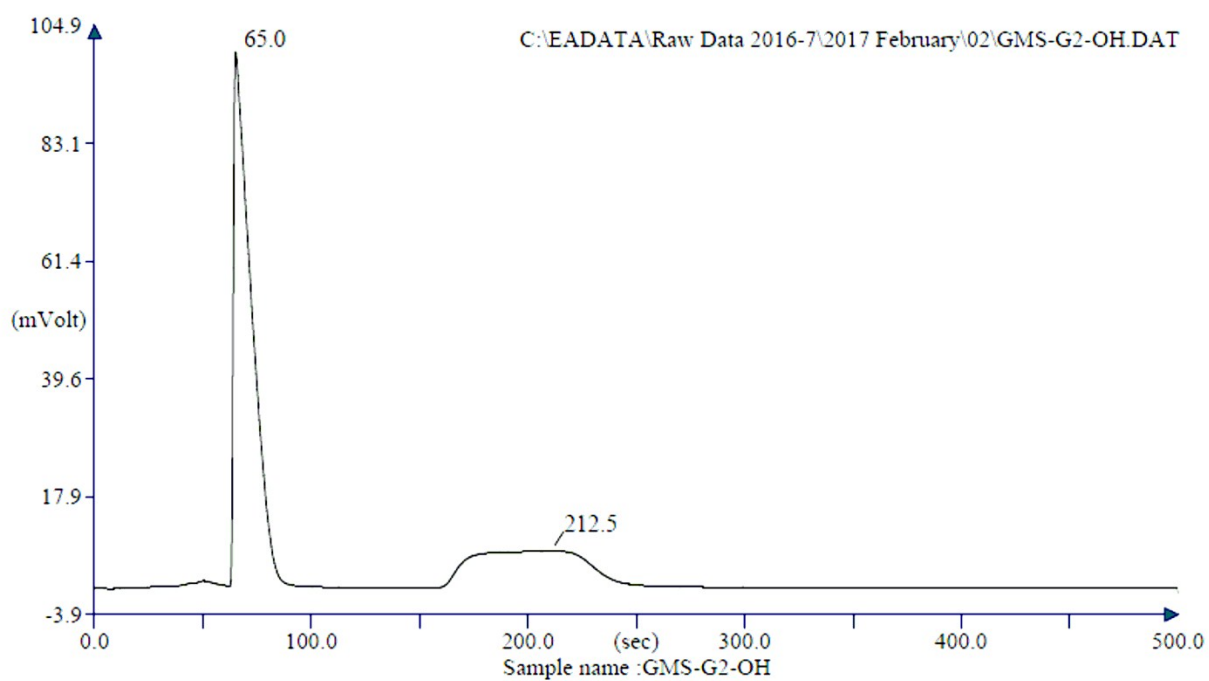
Retention Time (min)	Element Name	Element %
1.100	Carbon	55.879
3.392	Hydrogen	8.639
		64.518

**Fig. S3.** Elemental analysis chromatogram of GMOA-G2-OH.



Retention Time (min)	Element Name	Element %
1.117	Carbon	54.625
3.258	Hydrogen	7.869
		62.495

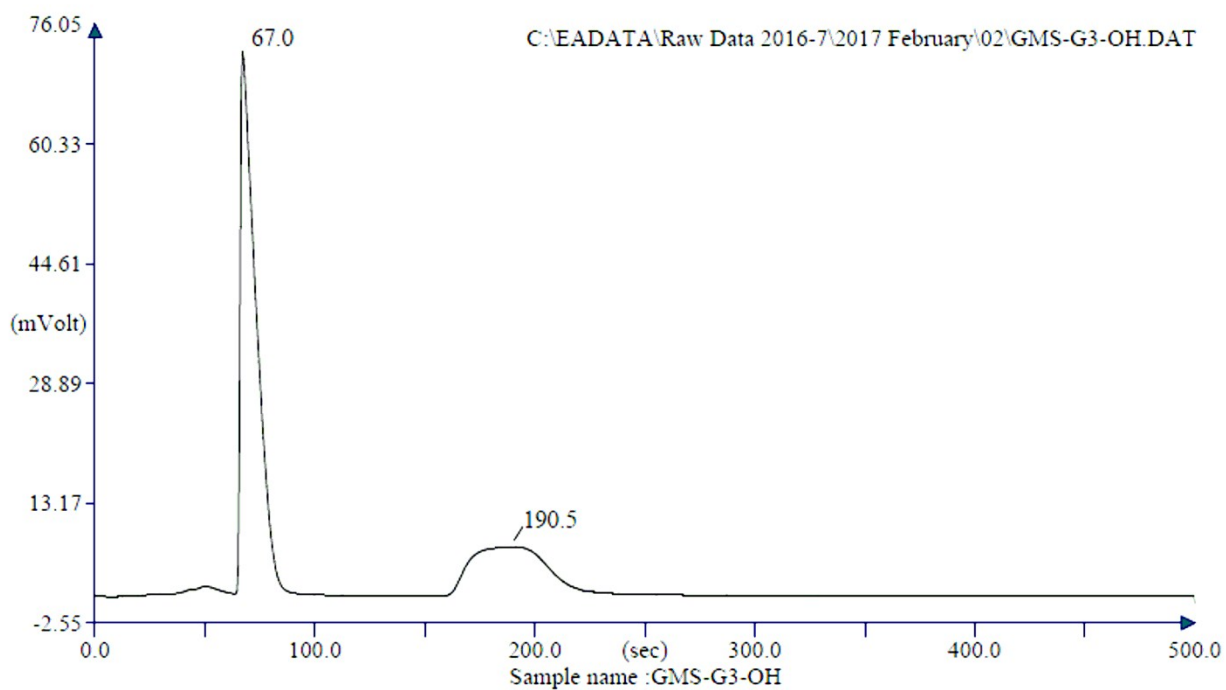
**Fig. S4.** Elemental analysis chromatogram of GMOA-G3-OH.



Retention Time (min)	Element Name	Element %
1.083	Carbon	57.314
3.542	Hydrogen	8.623
		65.937

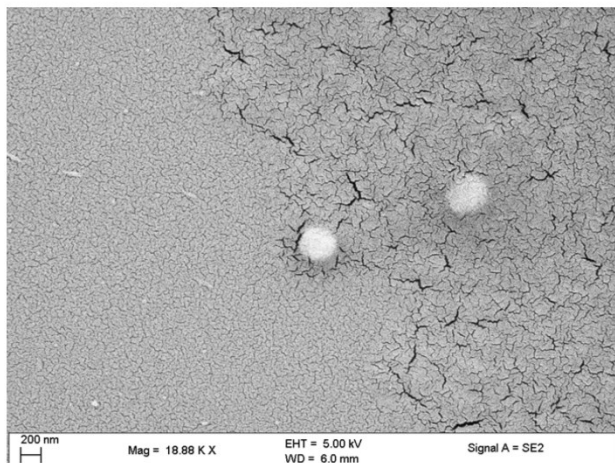
**Fig. S5.** Elemental analysis chromatogram of GMS-G2-OH.



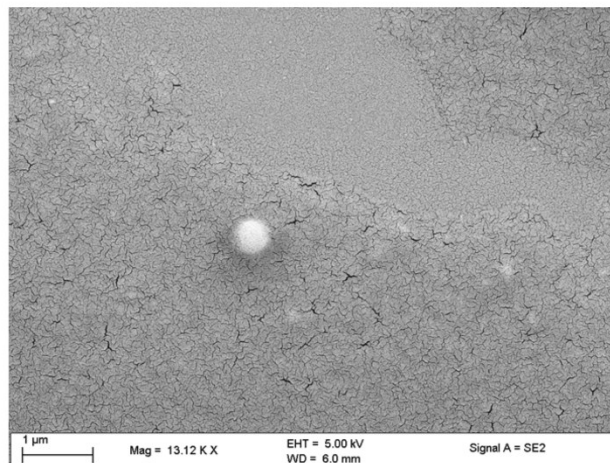


Retention Time (min)	Element Name	Element %
1.117	Carbon	55.082
3.175	Hydrogen	8.063
		<u>63.145</u>

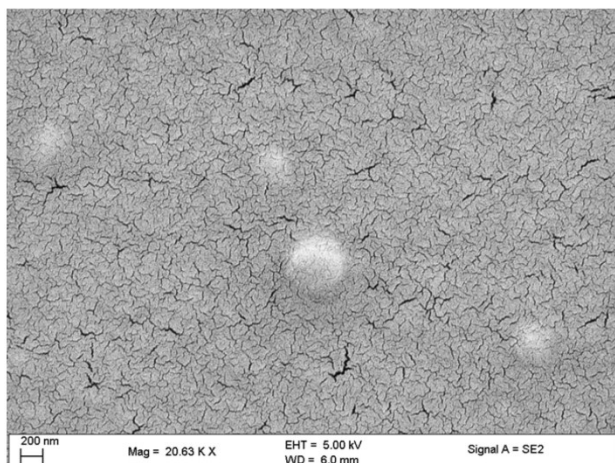
**Fig. S6.** Elemental analysis chromatogram of GMS-G3-OH.



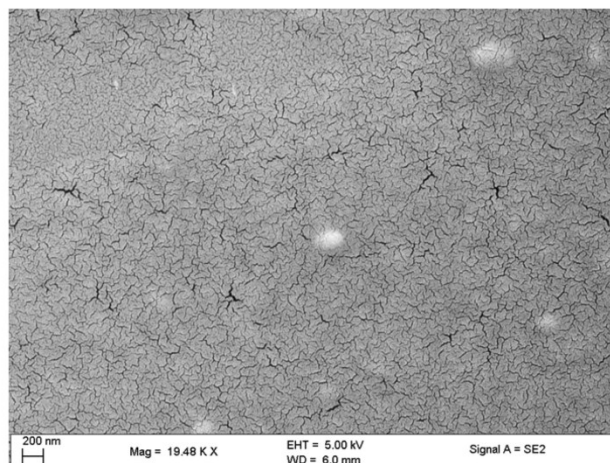
**A**



**B**



**C**



**D**

**Fig. S7.** SEM images showing morphology of SLNs stabilized using A) GMOA-G2-OH, B) GMS-G2-OH, C) GMOA-G3-OH and D) GMS-G3-OH ADs.

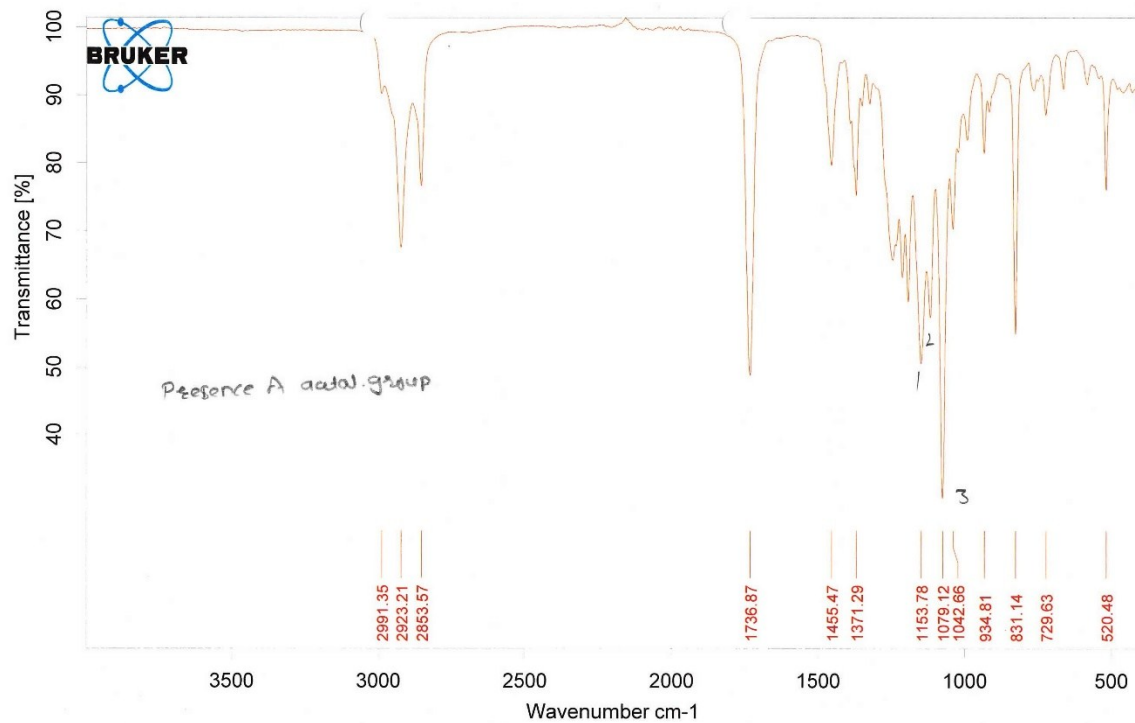


Fig. S8. FT-IR spectra of GMS-G1-Me.

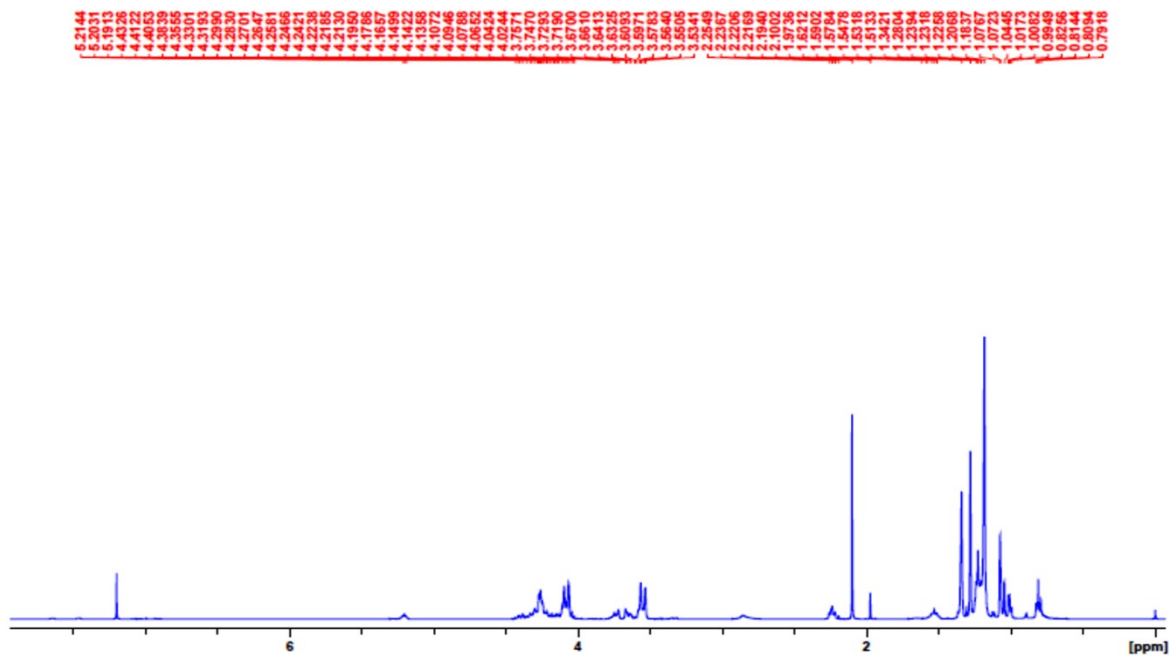


Fig. S9. <sup>1</sup>H NMR of GMS-G1-Me.

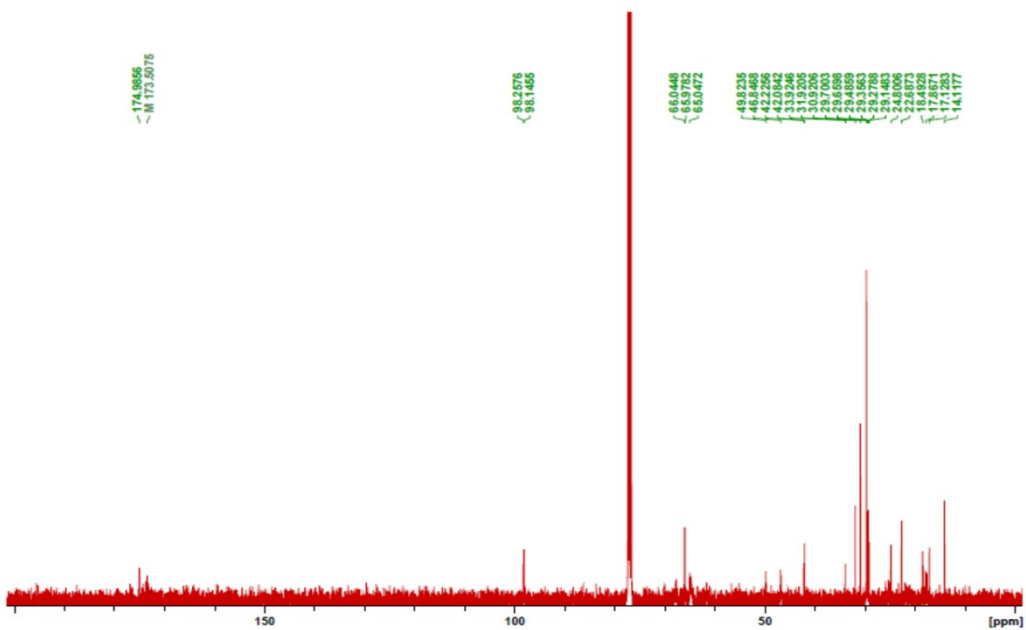


Fig. S10. <sup>13</sup>C NMR of GMS-G1-OH.

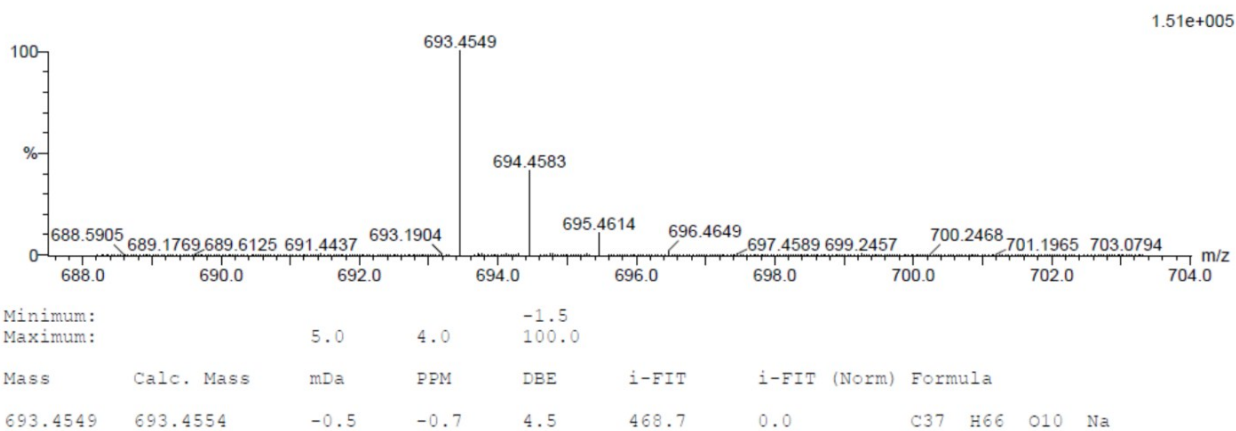


Fig. S11. HRMS of GMS-G1-Me.

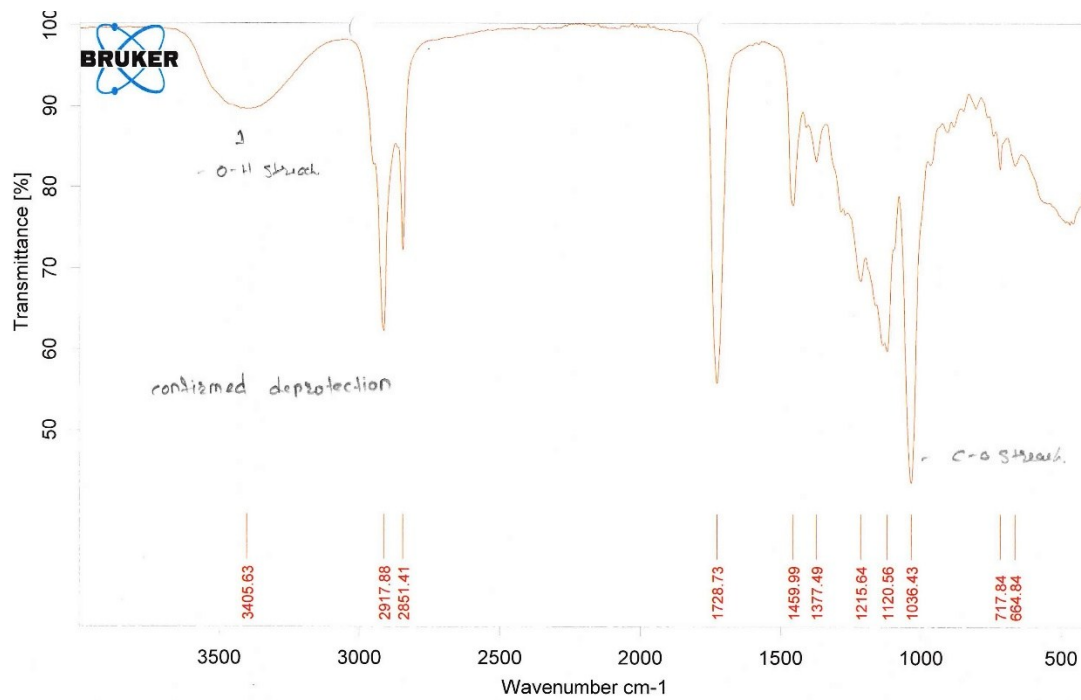


Fig. S12. FT-IR spectra of GMS-G1-OH.

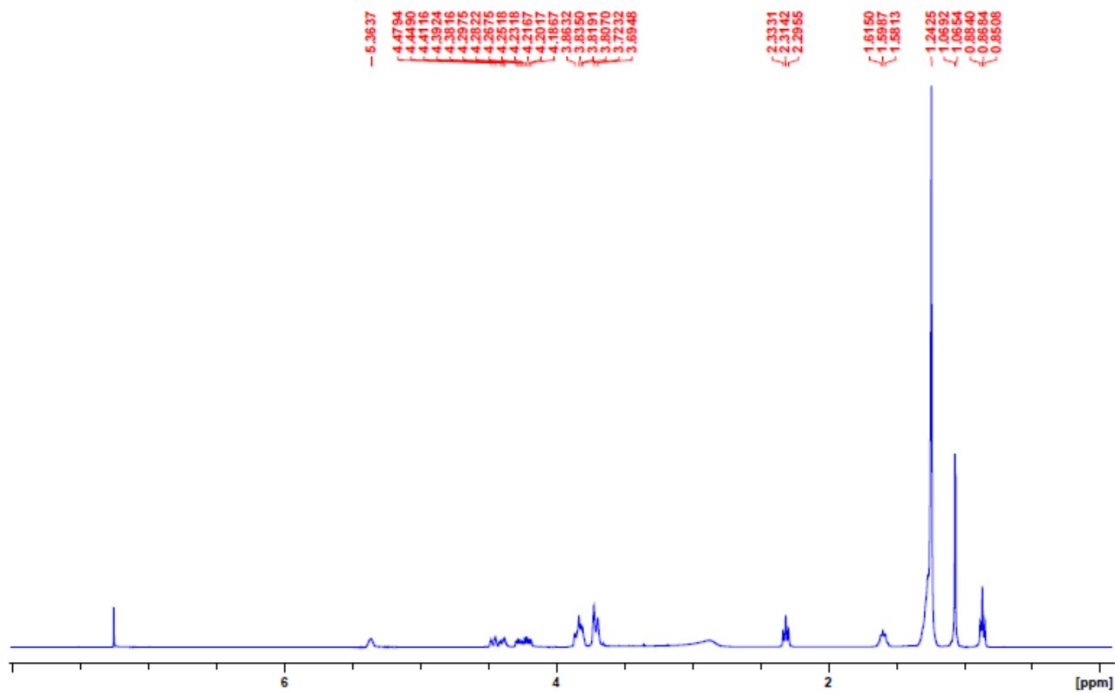


Fig. S13. <sup>1</sup>H NMR of GMS-G1-OH.

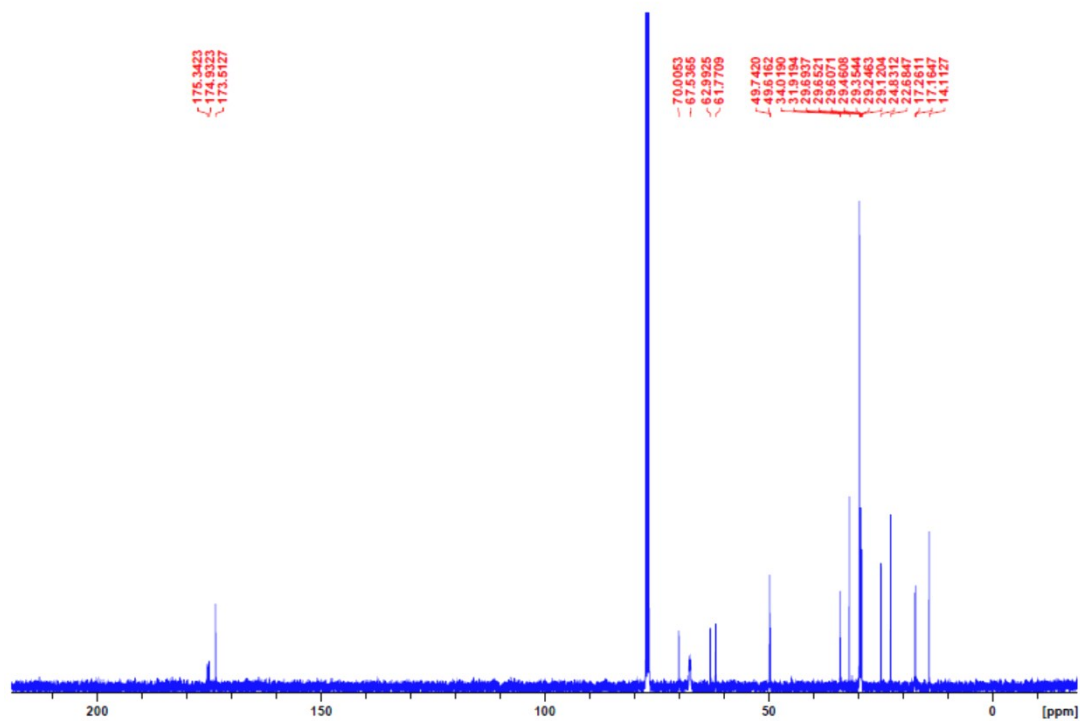


Fig. S14.  $^{13}\text{C}$  NMR of GMS-G1-OH.

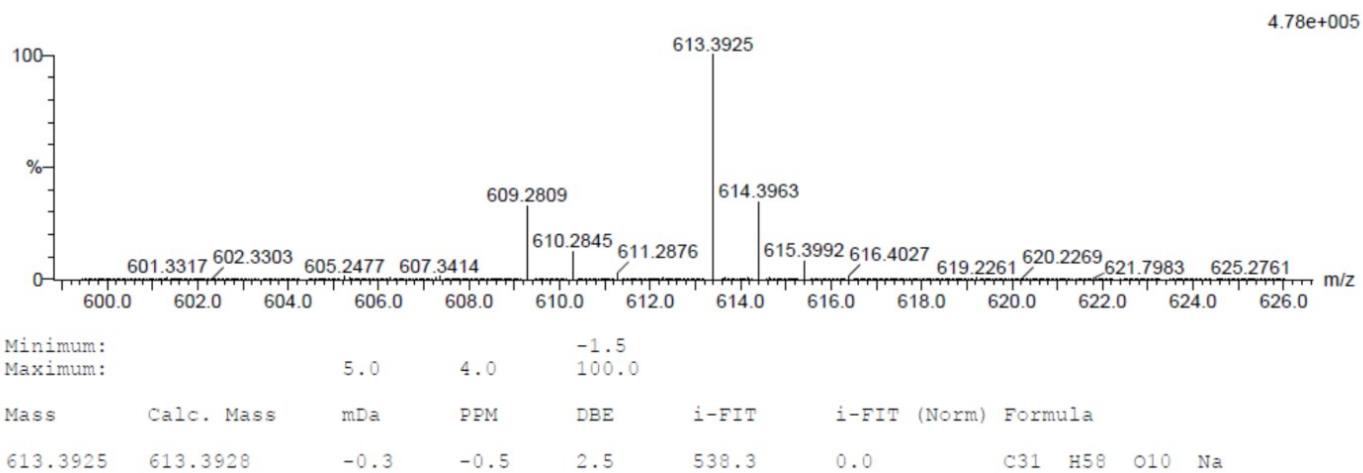


Fig. S15. HRMS of GMS-G1-OH.

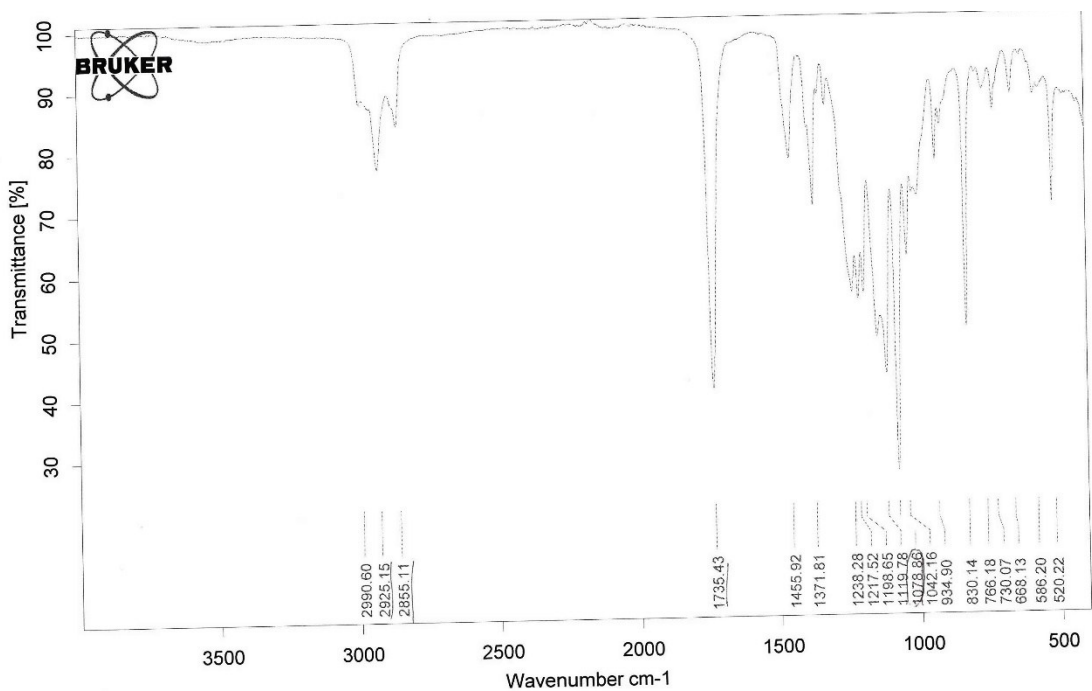


Fig. S16. FT-IR spectra of GMS-G2-Me.

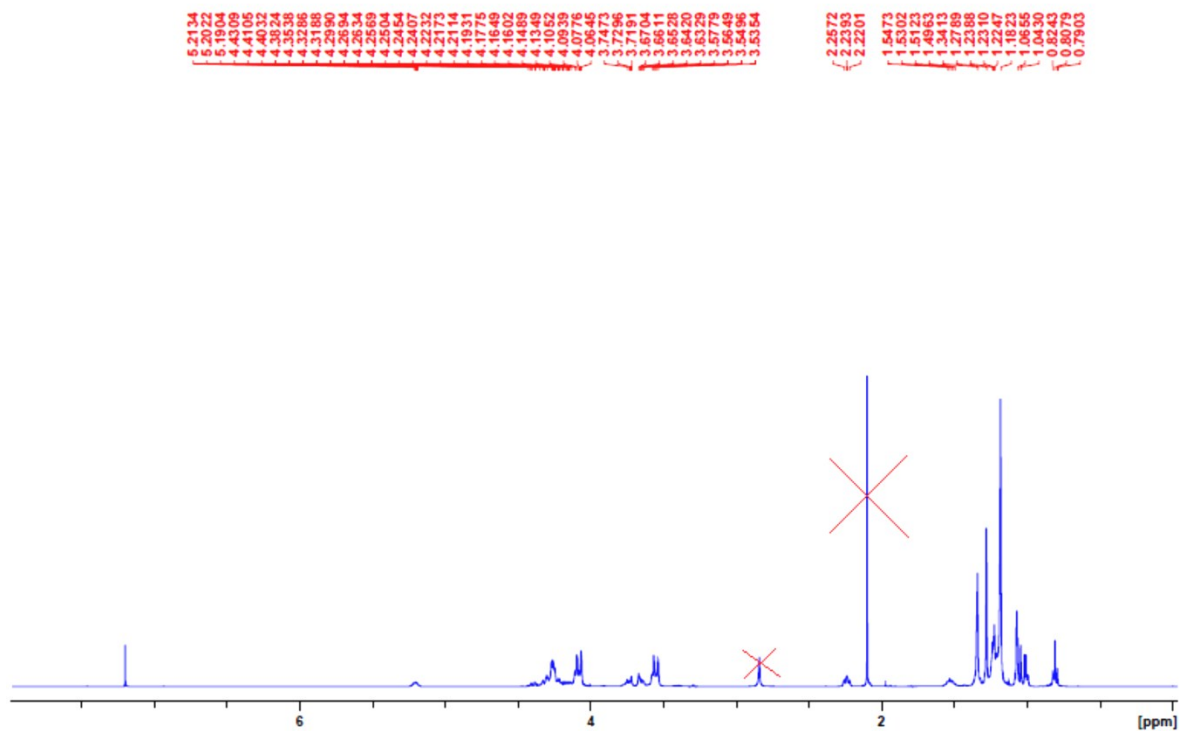


Fig. S17. <sup>1</sup>H NMR of GMS-G2-Me.

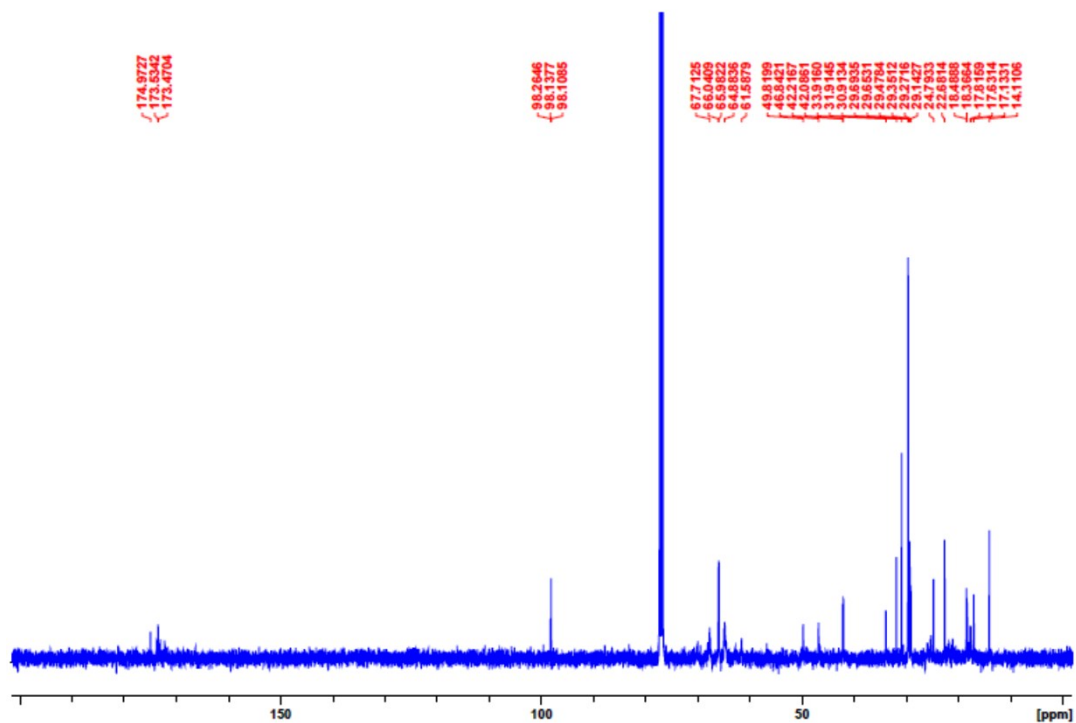


Fig. S18.  $^{13}\text{C}$  NMR of GMS-G2-Me.

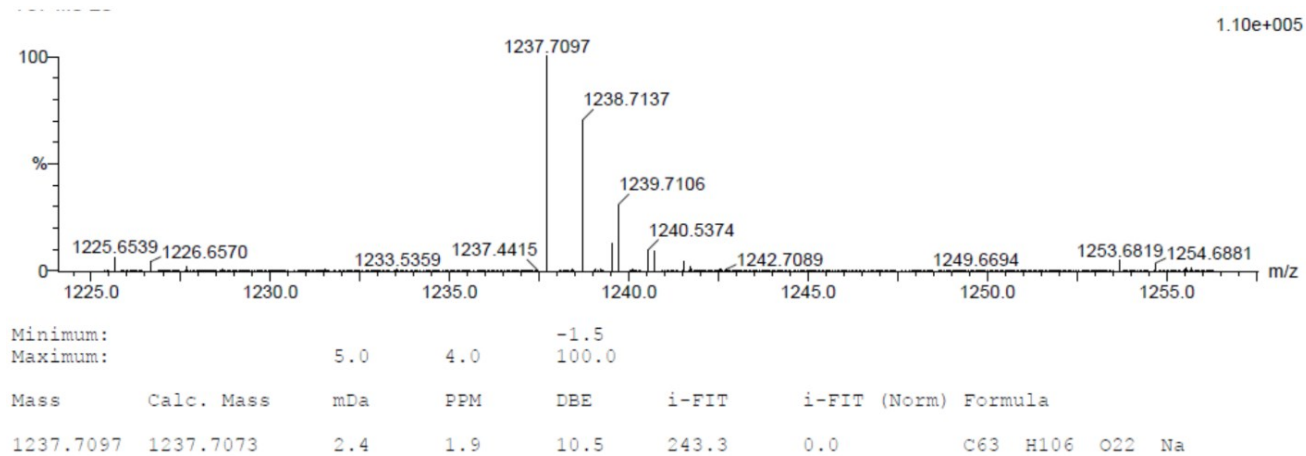


Fig. S19. HRMS of GMS-G2-Me.



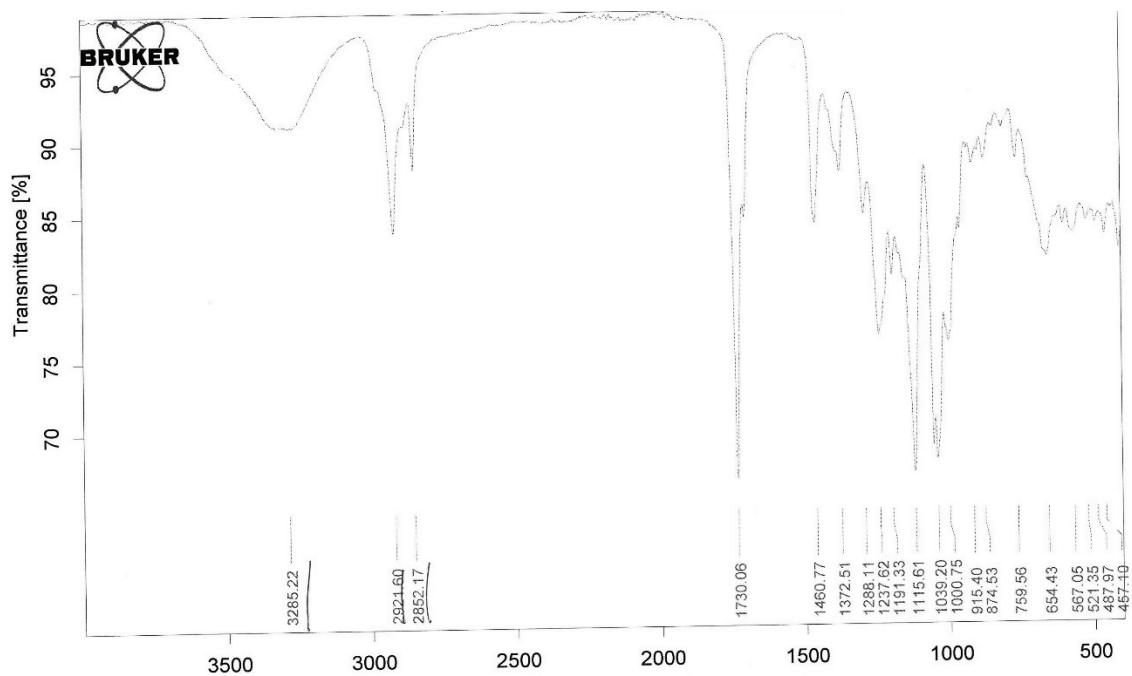


Fig. S20. FT-IR spectra of GMS-G2-OH.

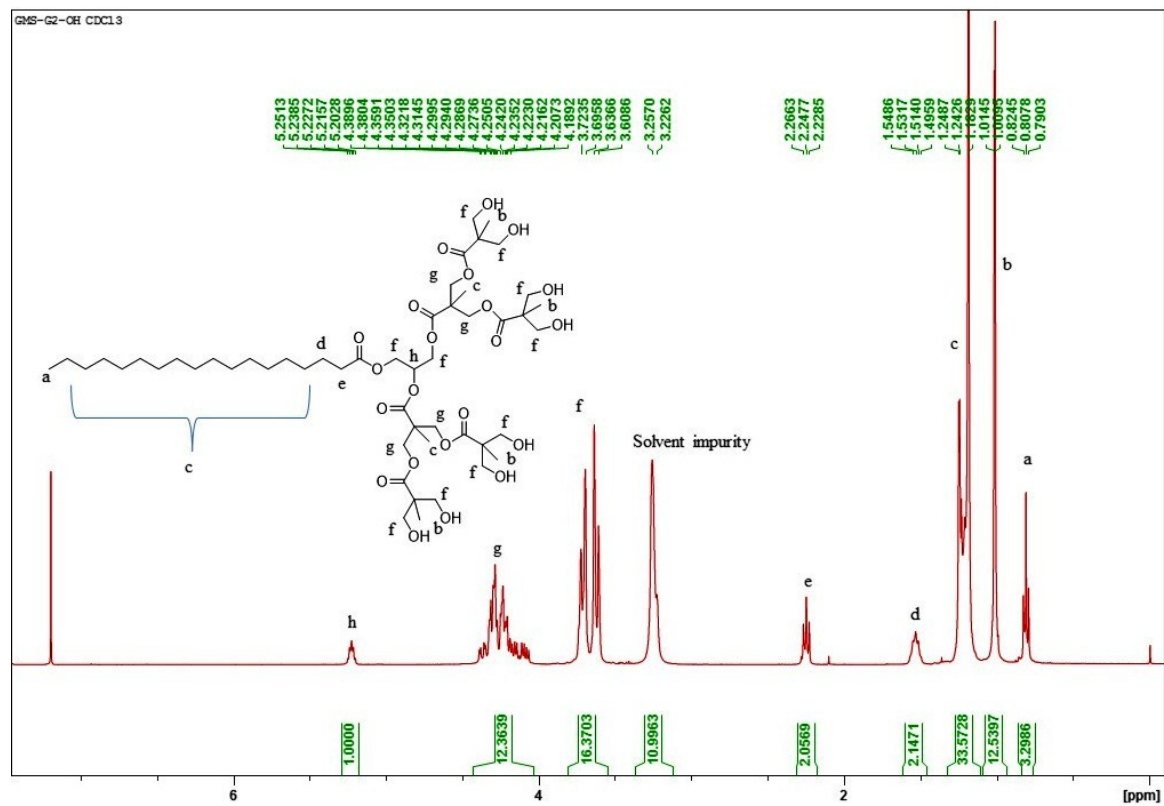


Fig. S21. <sup>1</sup>H NMR of GMS-G2-OH.

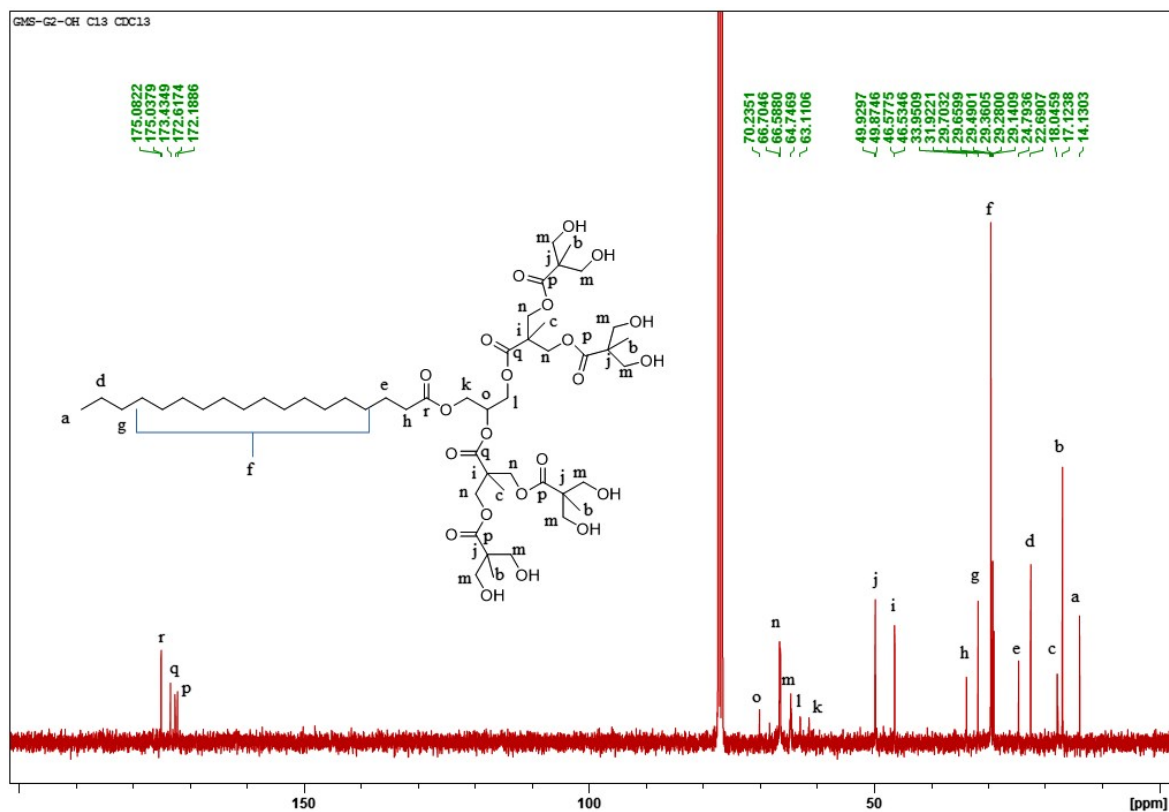


Fig. S22.  $^{13}\text{C}$  NMR of GMS-G2-OH.

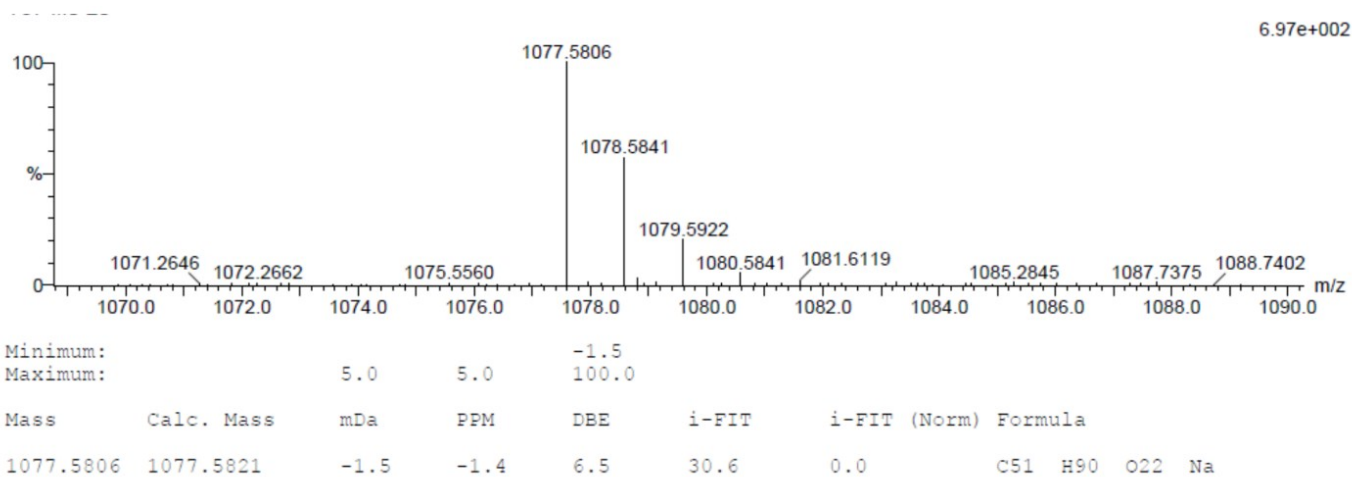


Fig. S23. HRMS of GMS-G2-OH.

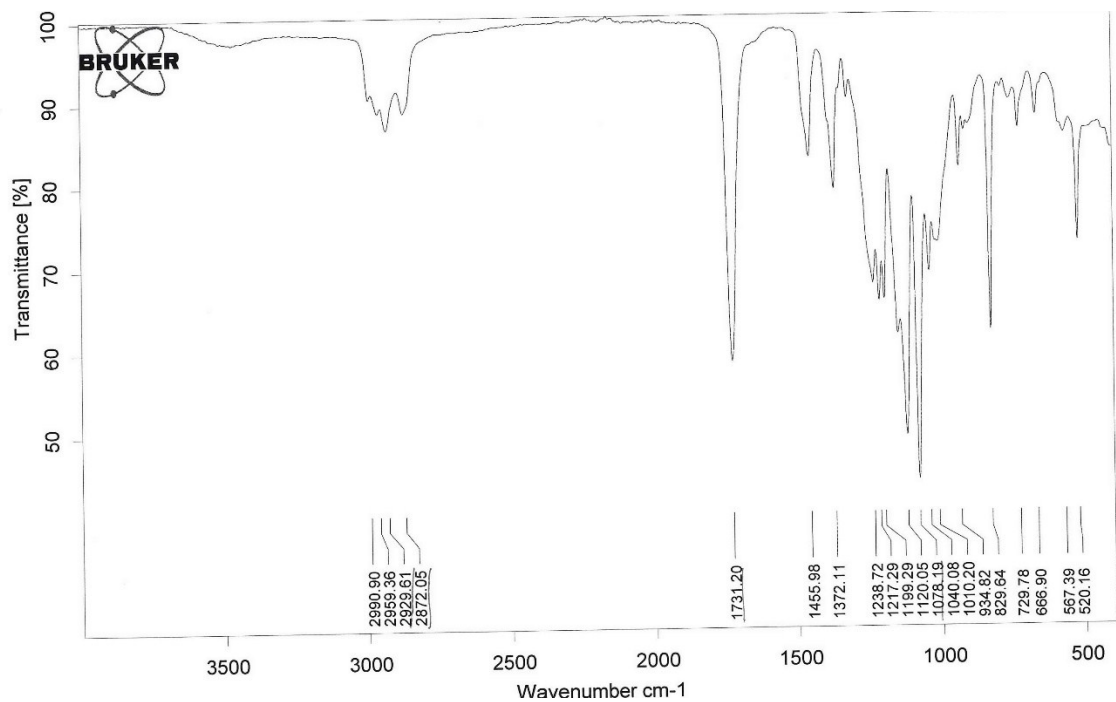


Fig. S24. FT-IR spectra of GMS-G3-Me.

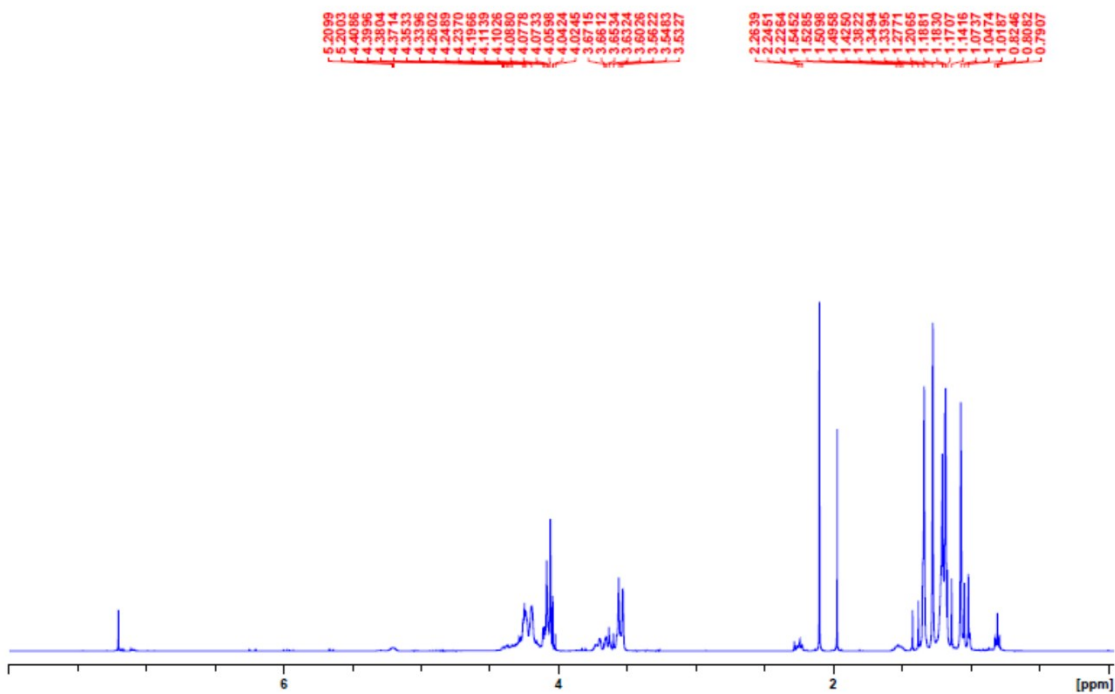
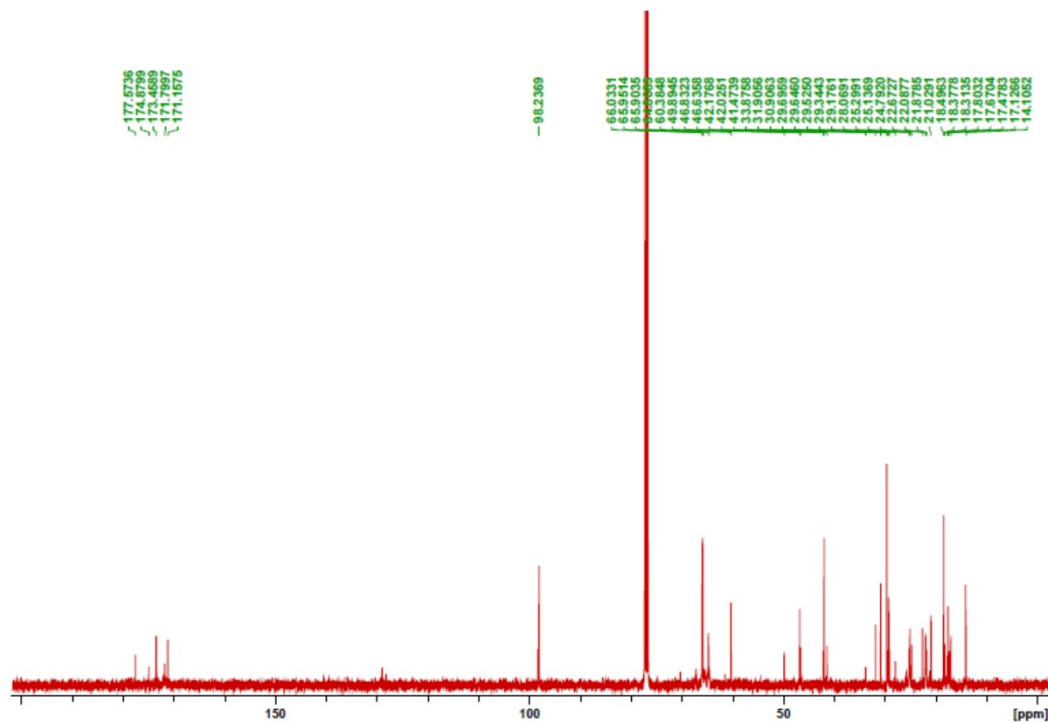
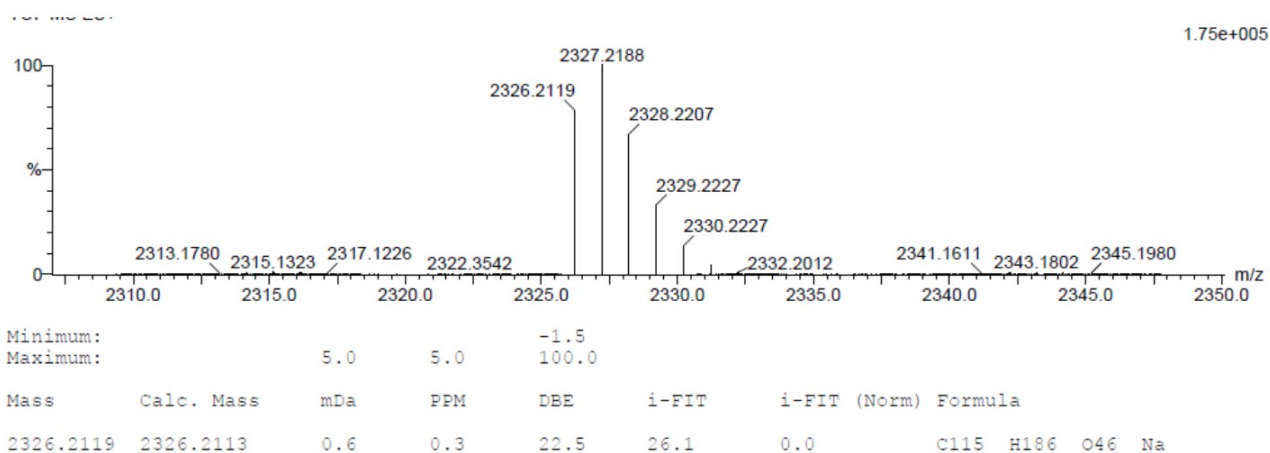


Fig. S25. <sup>1</sup>H NMR of GMS-G3-Me.



**Fig. S26.** <sup>13</sup>C NMR of GMS-G3-Me.



**Fig. S27.** HRMS of GMS-G3-Me.

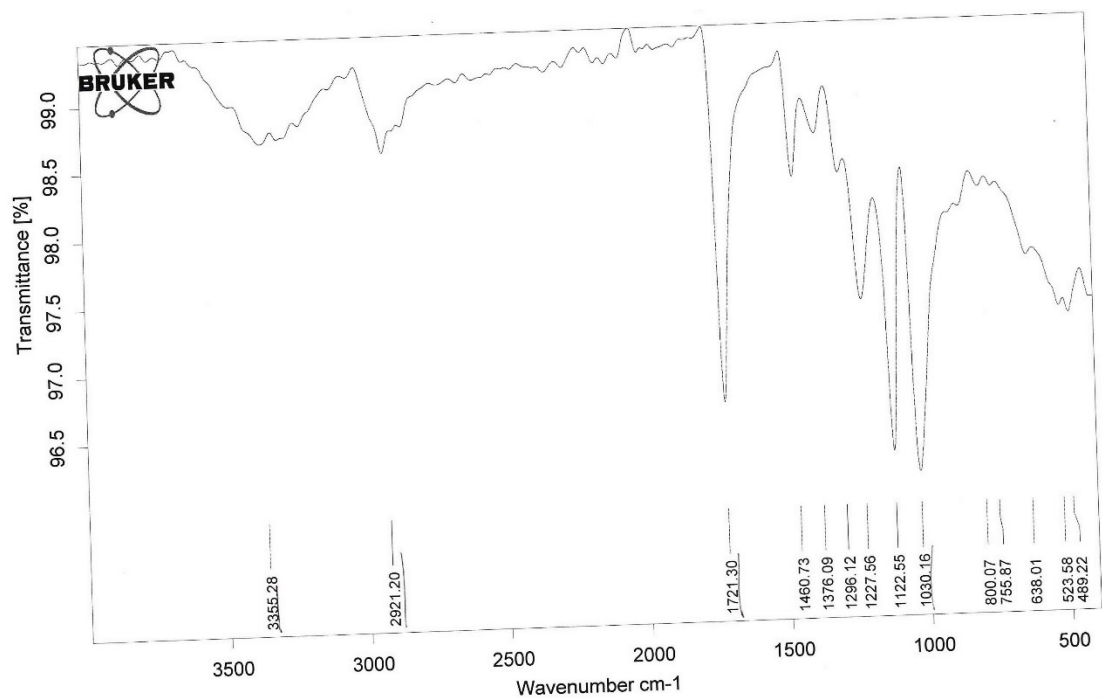


Fig. S28. FT-IR spectra of GMS-G3-Me.

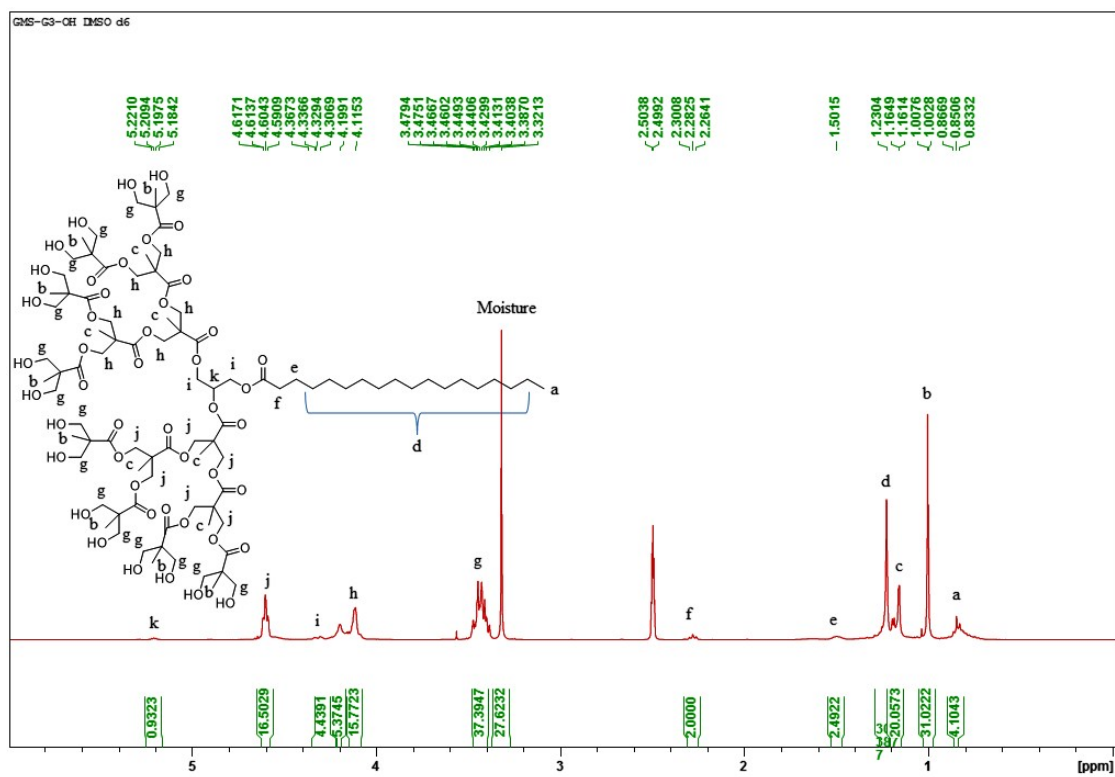


Fig. S29. <sup>1</sup>H NMR of GMS-G3-OH.

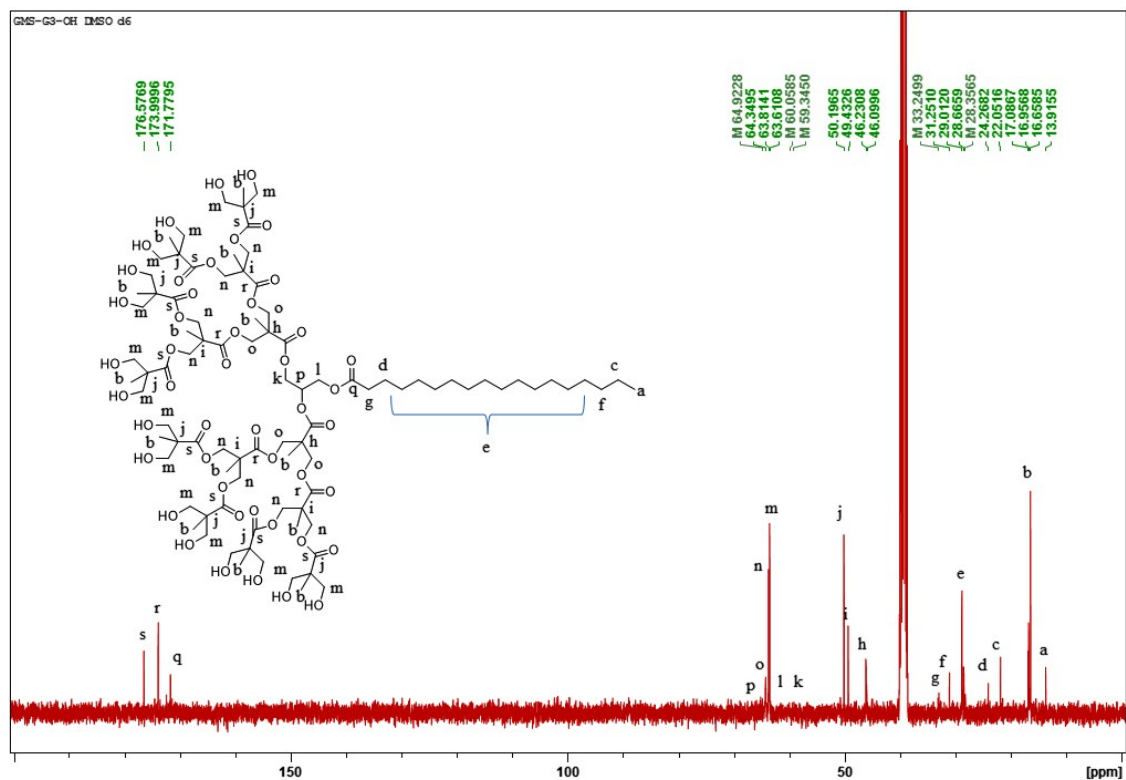


Fig. S30.  $^{13}\text{C}$  NMR of GMS-G3-OH.

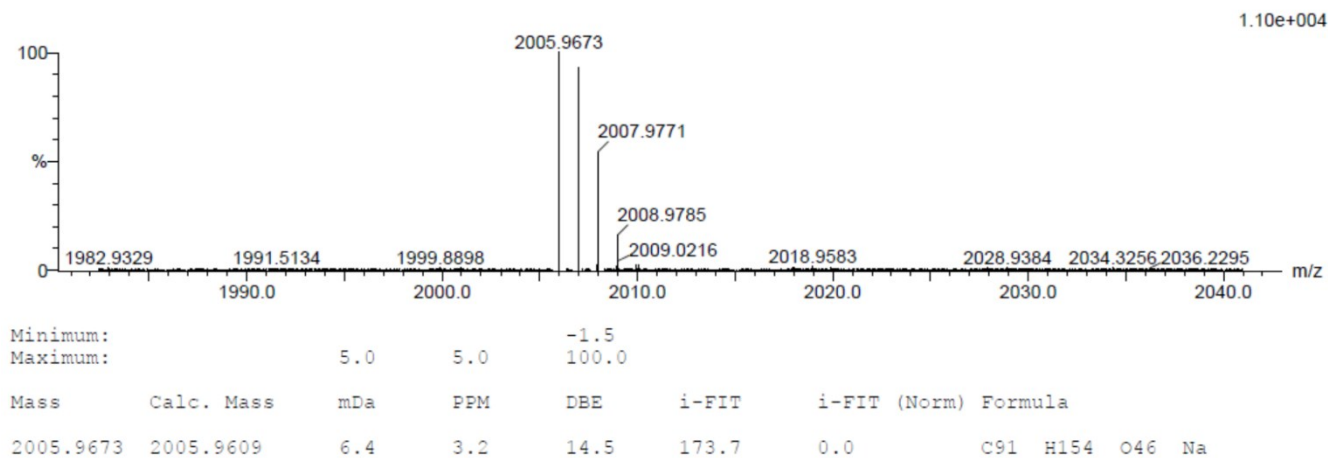


Fig. S31. HRMS of GMS-G3-OH.

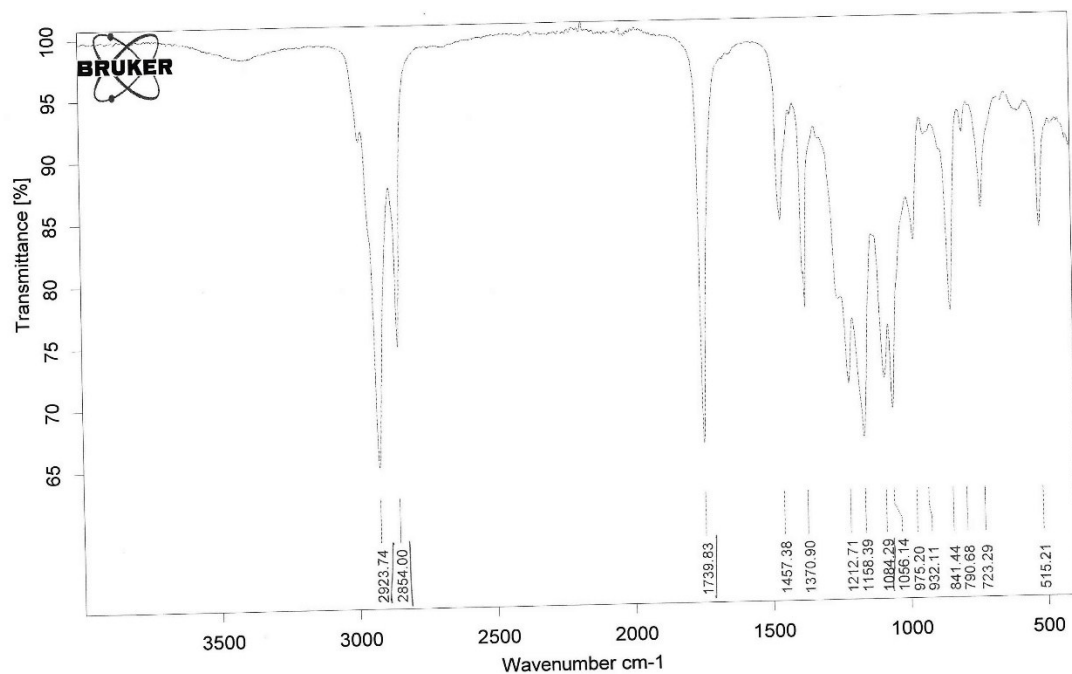


Fig. S32. FT-IR spectra of GMOA-Me.

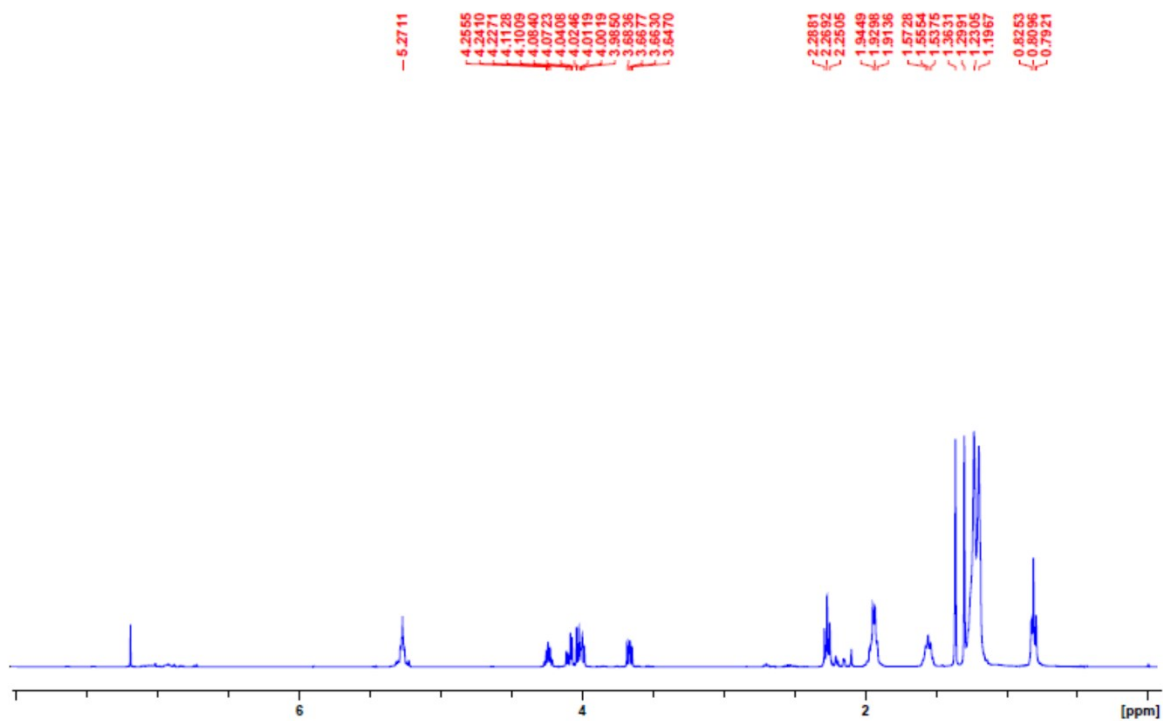


Fig. S33. <sup>1</sup>H NMR of GMOA-Me.

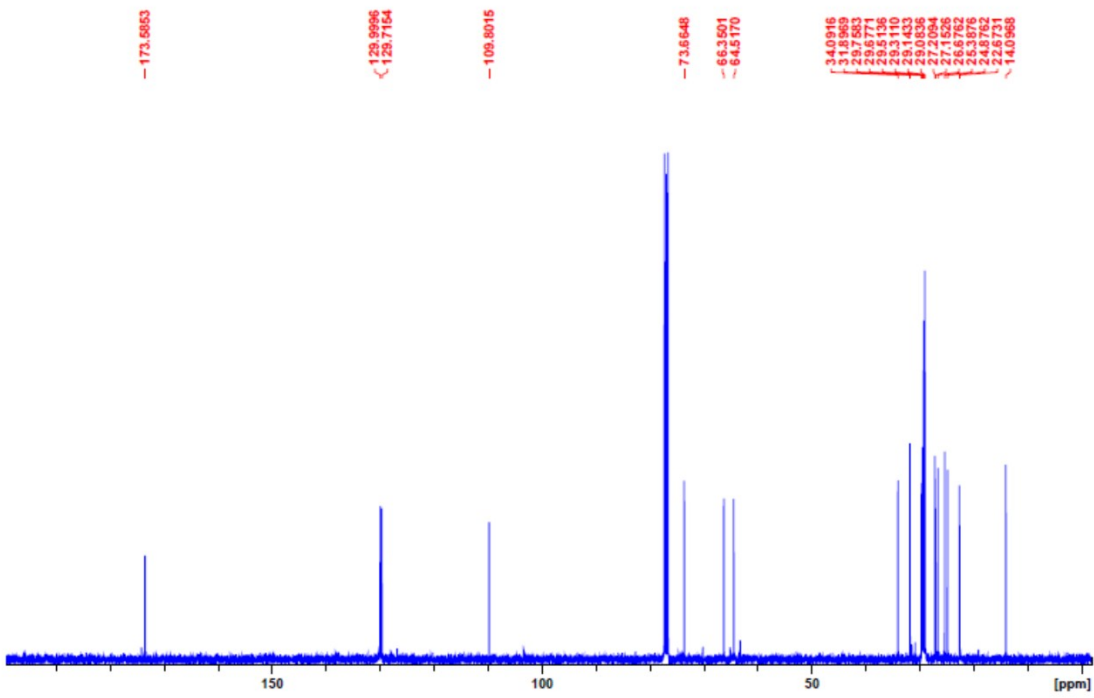


Fig. S34.  $^{13}\text{C}$  NMR of GMOA-Me.

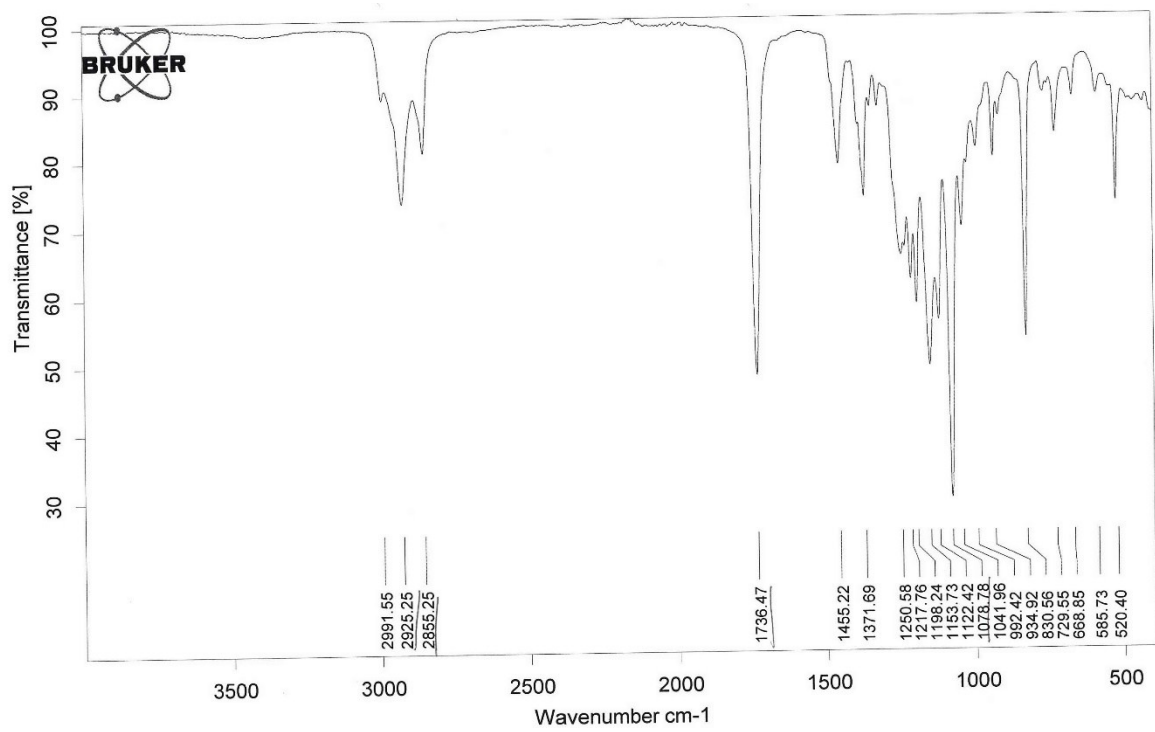


Fig. S35. FT-IR spectra of GMOA.



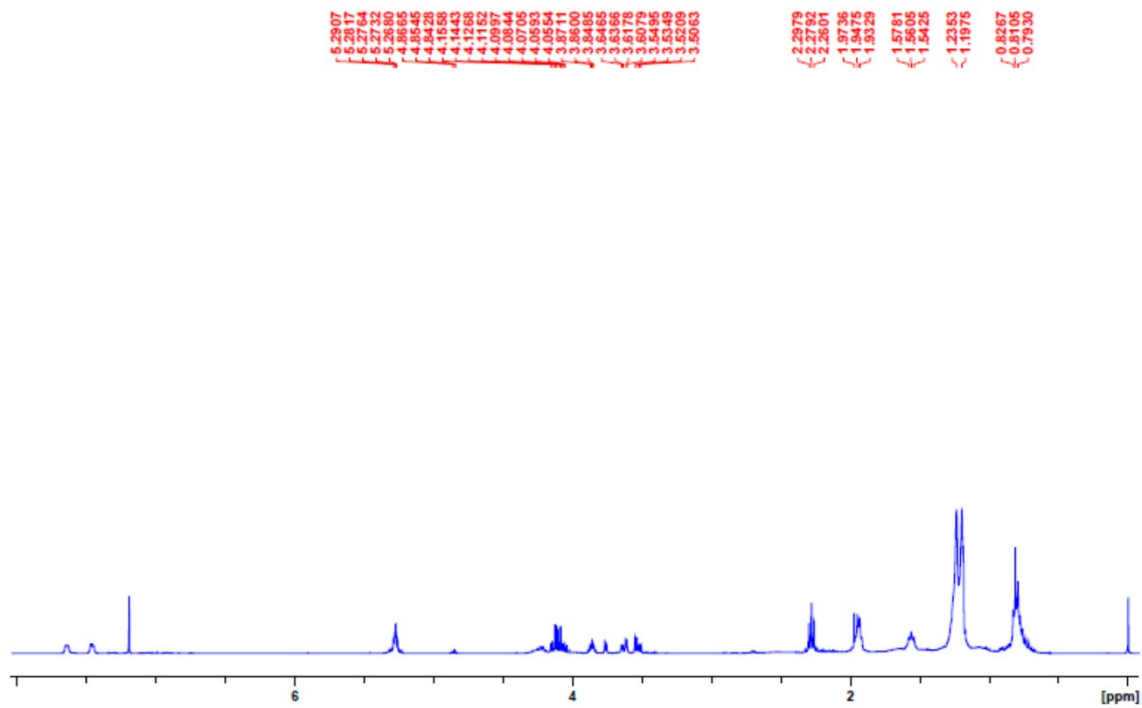


Fig. S36.  $^1\text{H}$  NMR of GMOA.

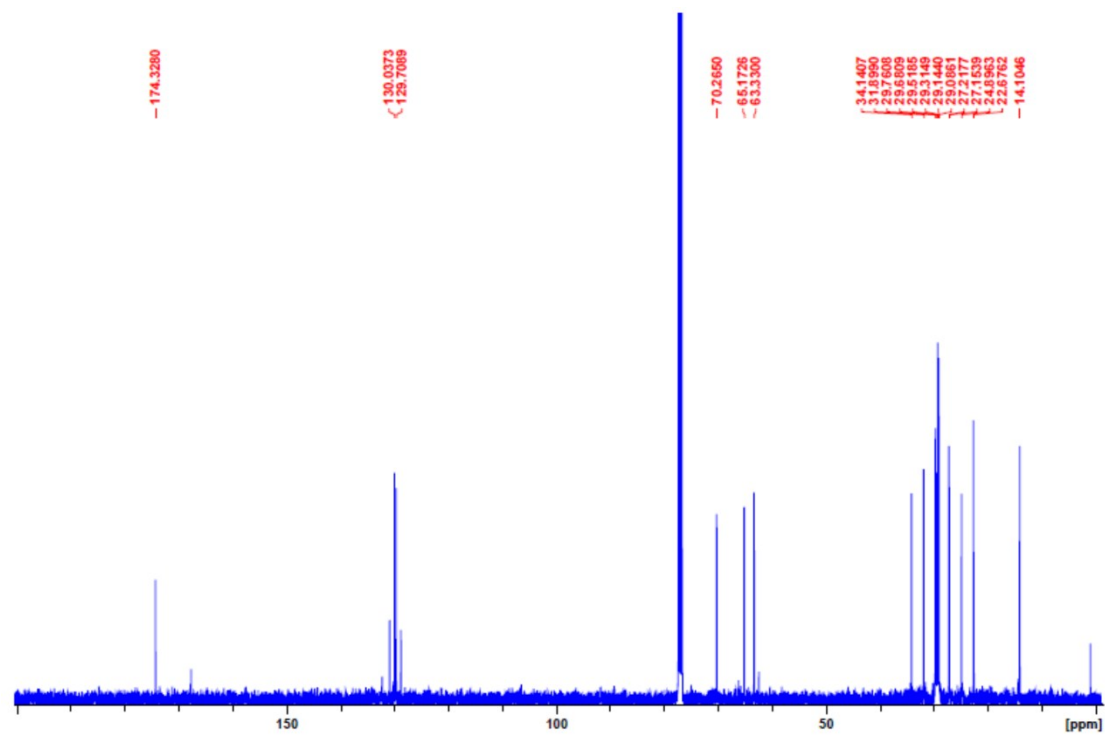


Fig. S37.  $^{13}\text{C}$  NMR of GMOA-OH.

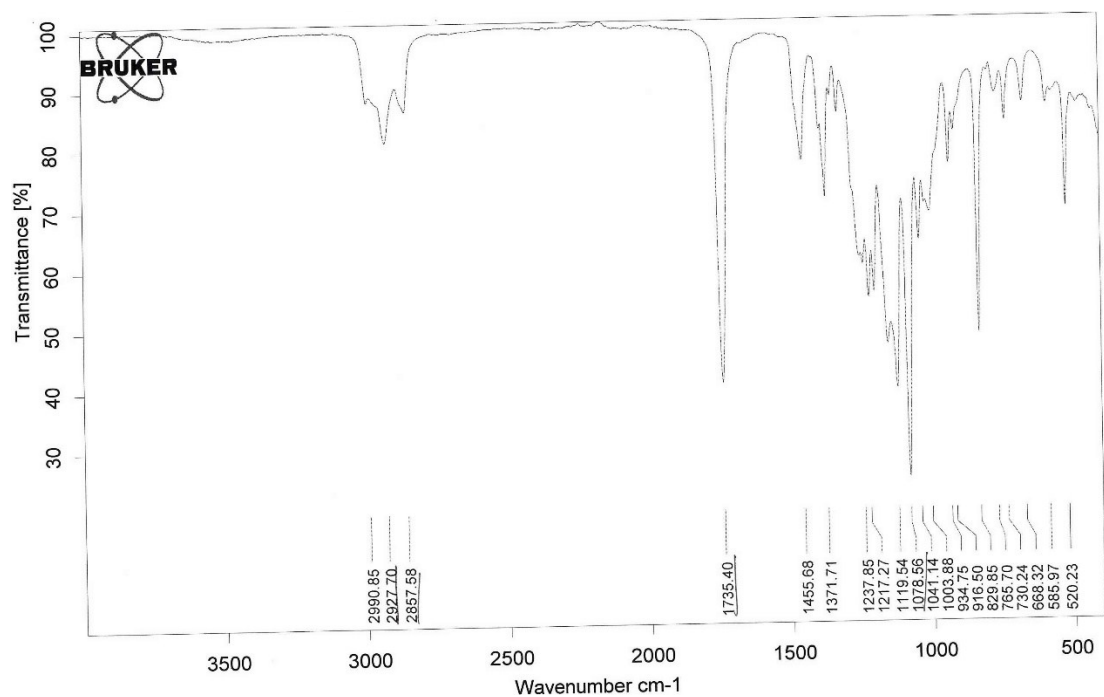


Fig. S38. FT-IR spectra of GMOA-G1-Me.

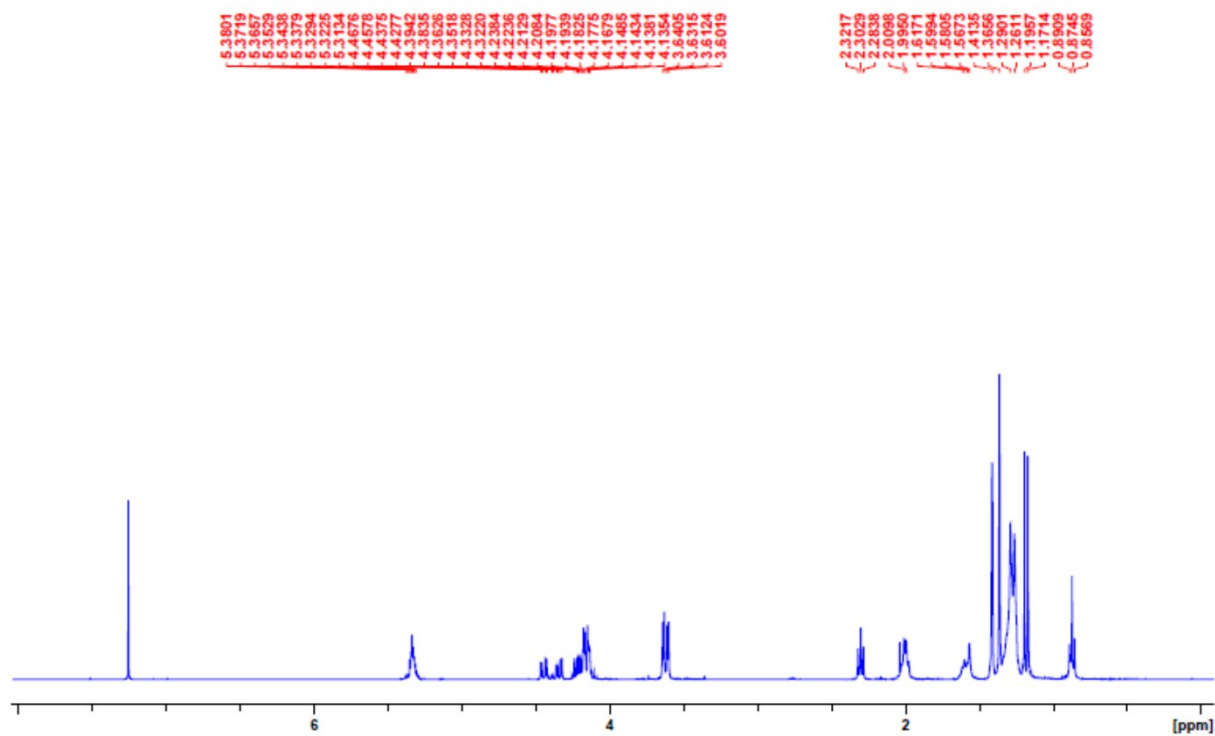


Fig. S39. <sup>1</sup>H NMR of GMOA-G1-Me.

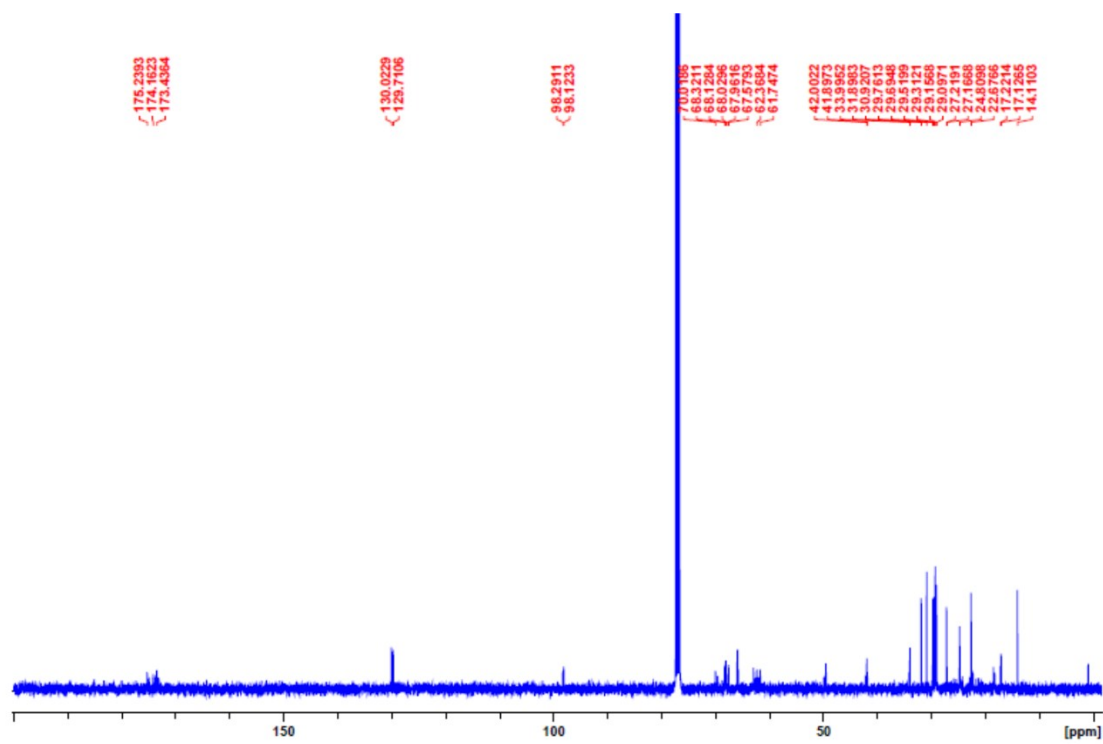


Fig. S40.  $^{13}\text{C}$  NMR of GMOA-G1-Me.

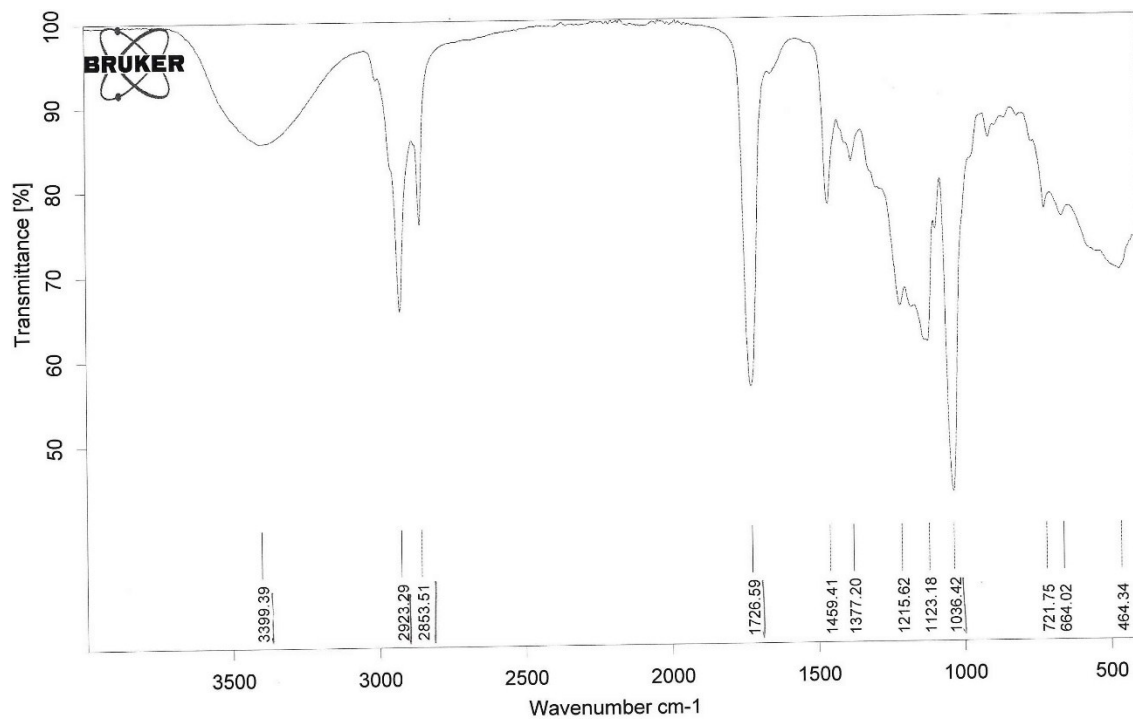


Fig. S41. FT-IR spectra of GMOA-G1-OH.

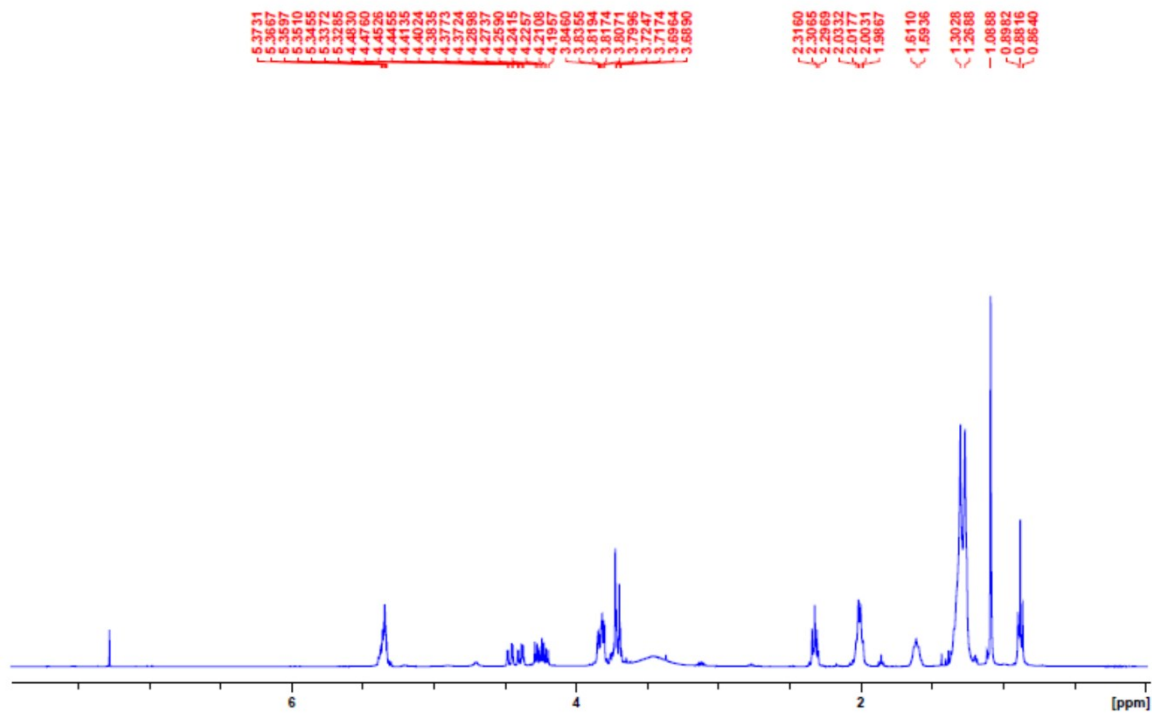


Fig. S42.  $^1\text{H}$  NMR of GMOA-G1-OH.

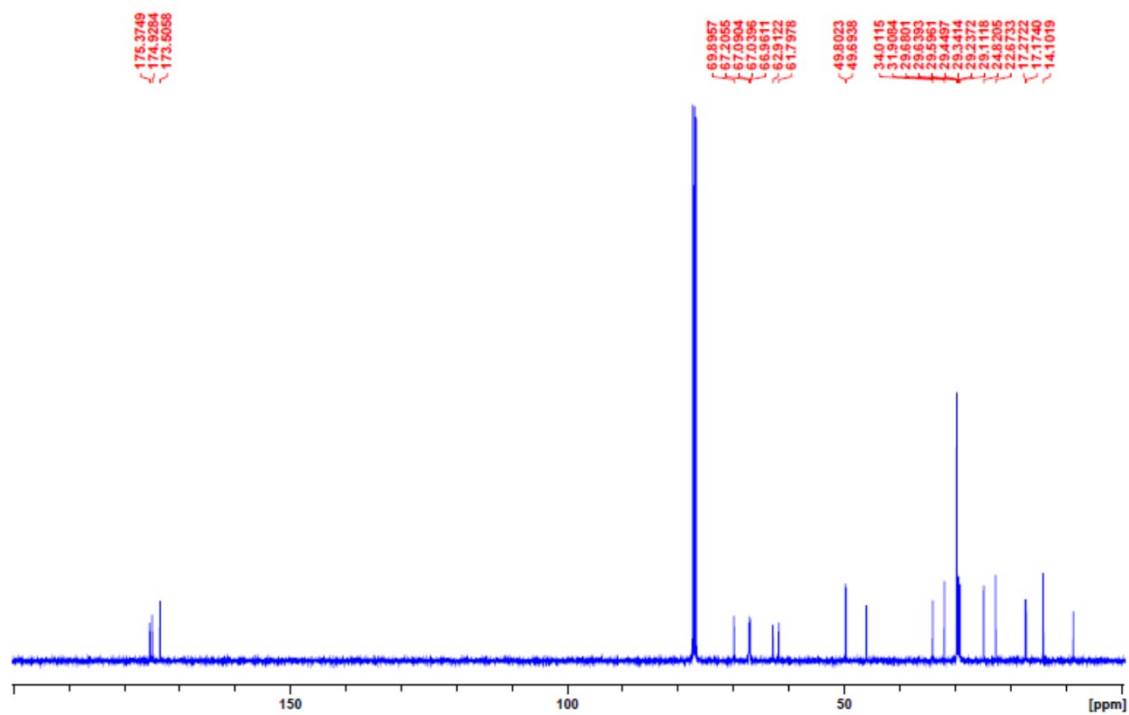
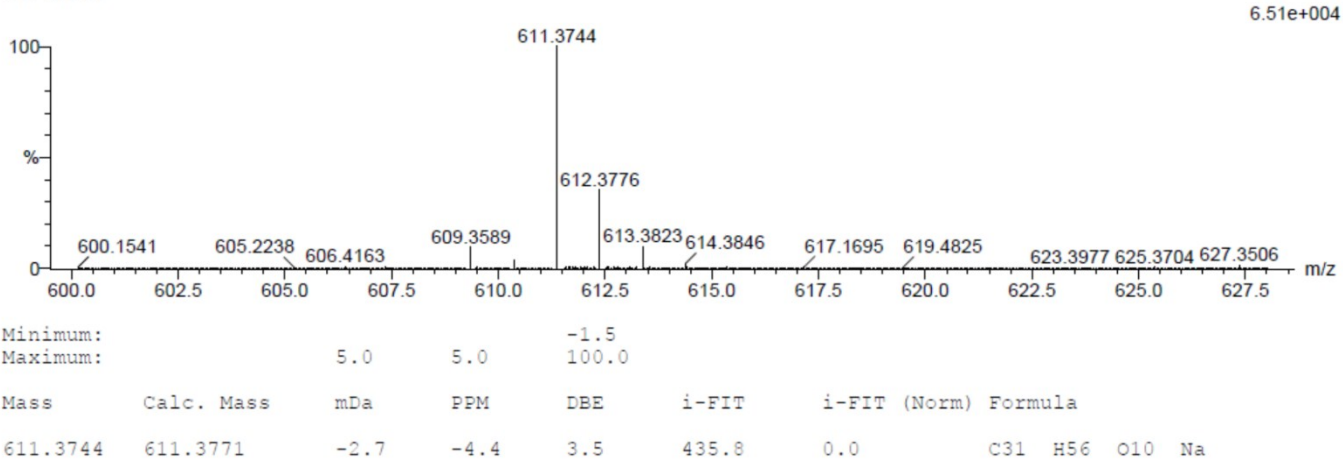
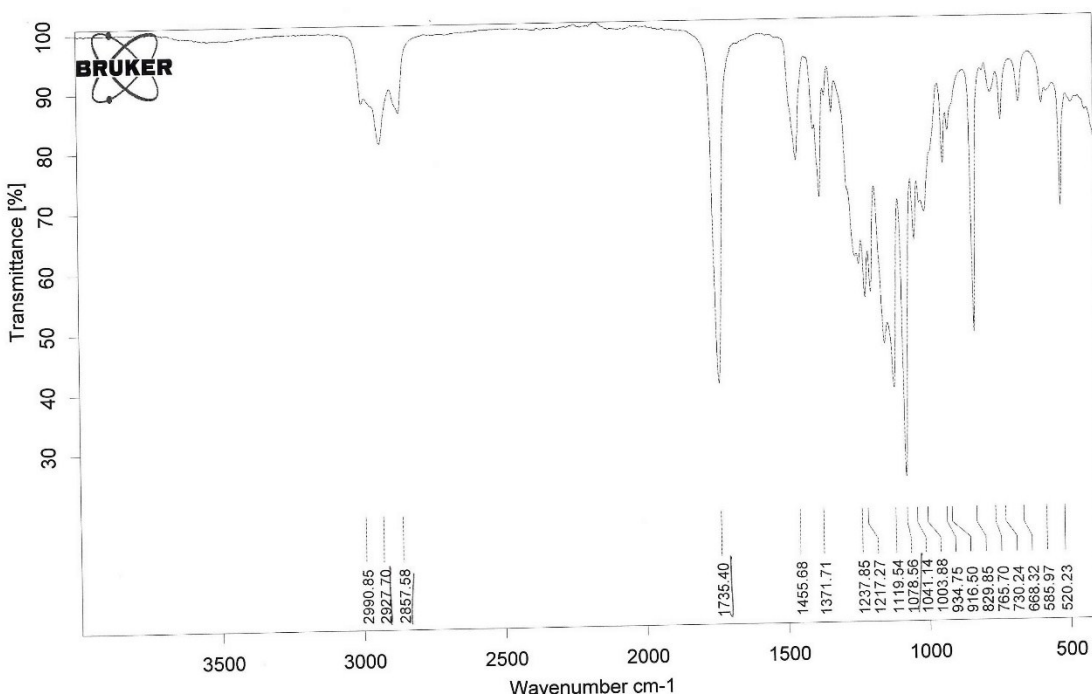


Fig. S43.  $^{13}\text{C}$  NMR of GMOA-G1-OH.



**Fig. S44.** HRMS of GMOA-G1-OH.



**Fig. S45.** FT-IR spectra of GMOA-G2-Me.

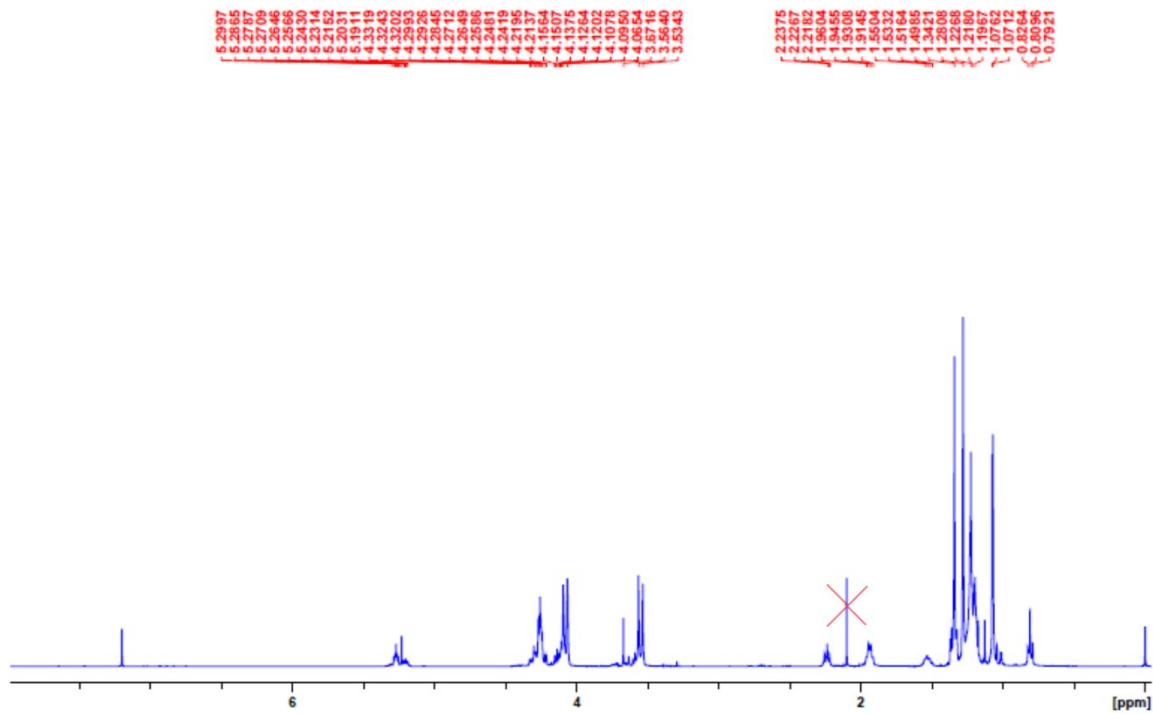


Fig. S46.  $^1\text{H}$  NMR of GMOA-G2-Me.

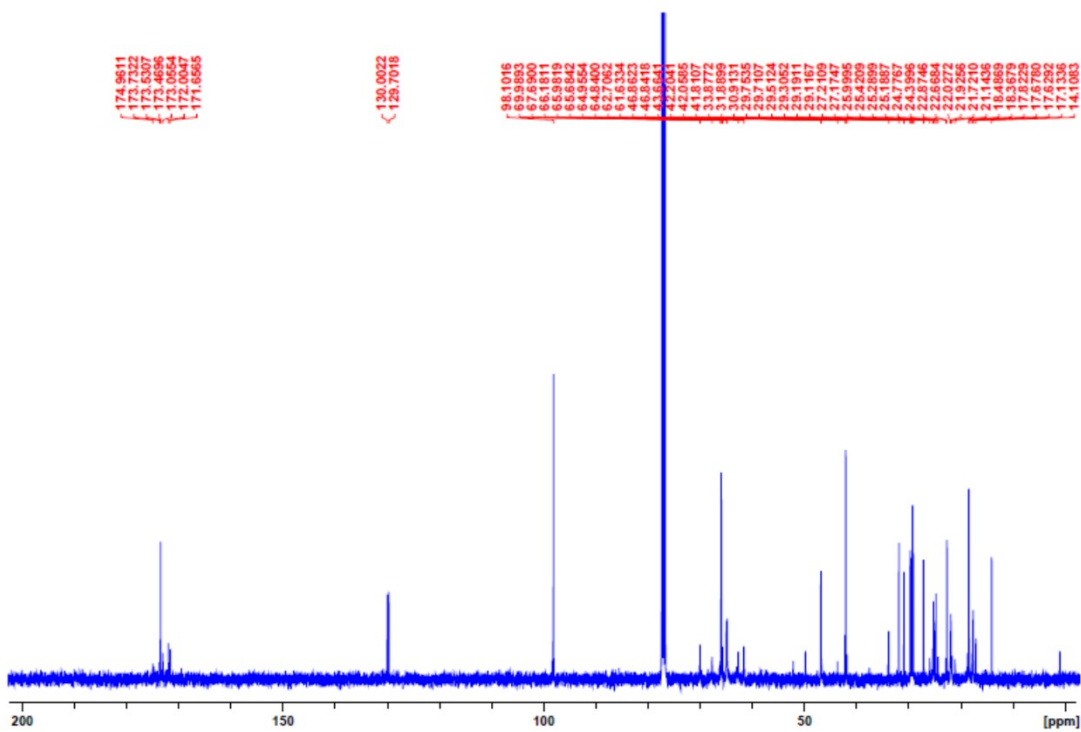


Fig. S47.  $^{13}\text{C}$  NMR of GMOA-G2-Me.

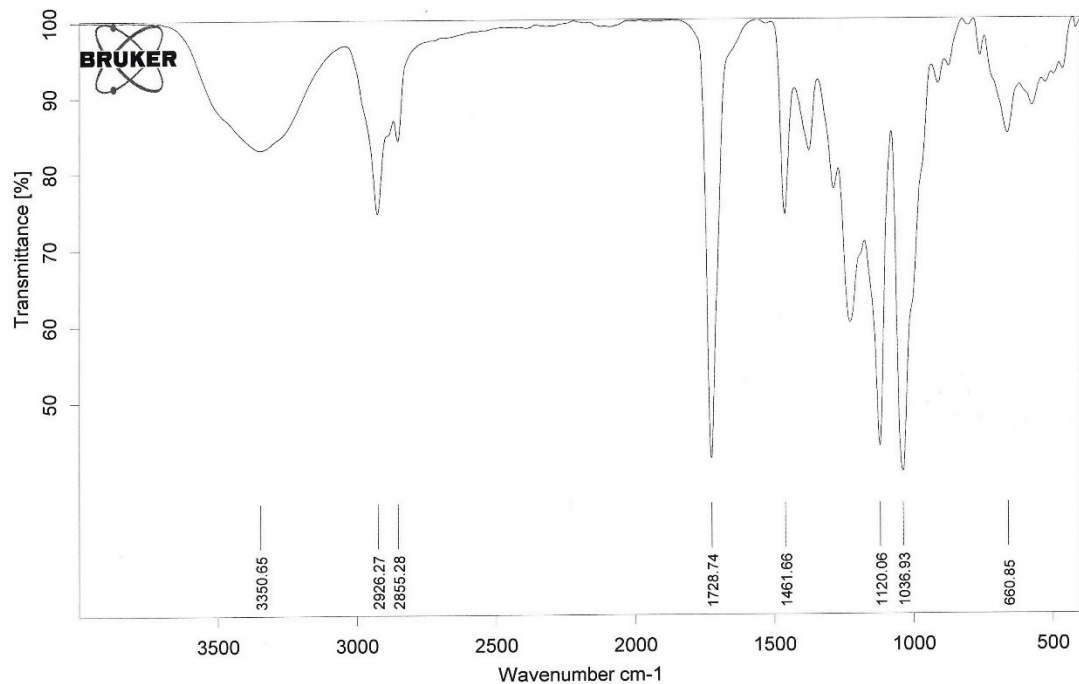


Fig. S48. FT-IR spectra of GMOA-G2-OH.

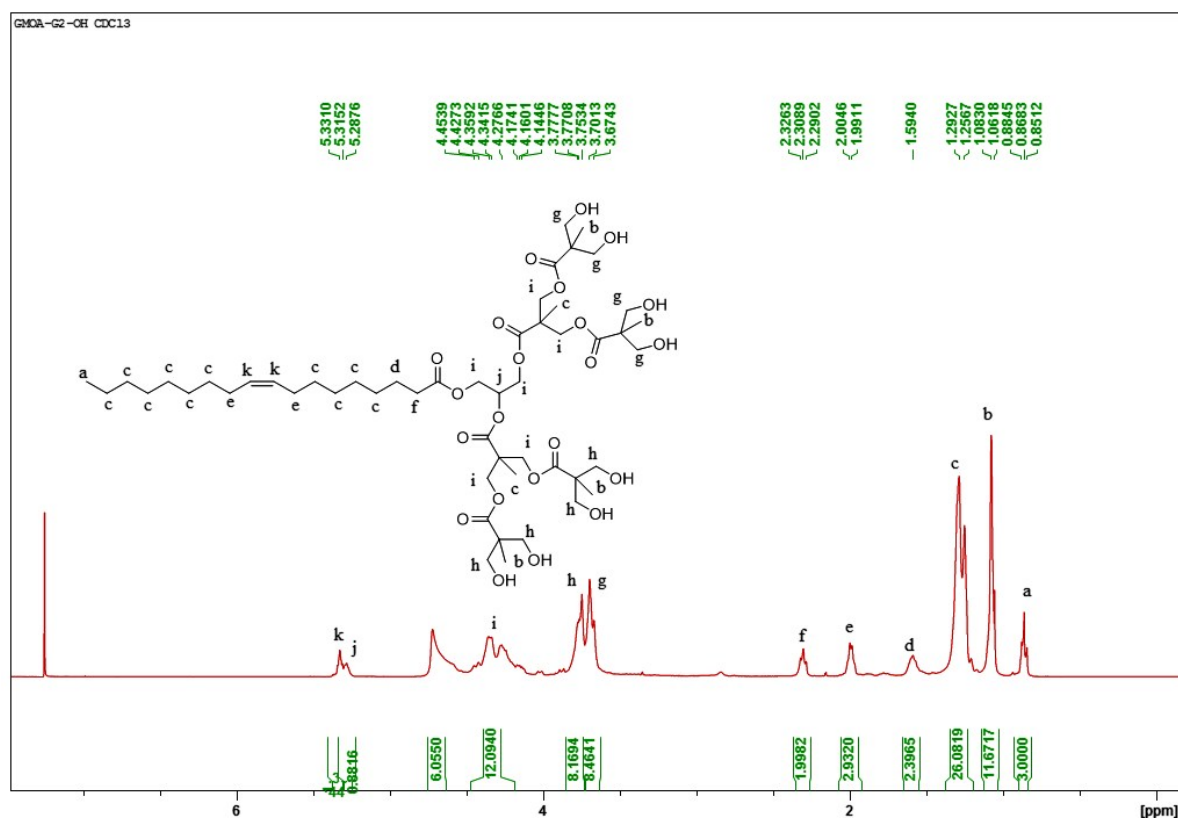


Fig. S49. <sup>1</sup>H NMR of GMOA-G2-OH.

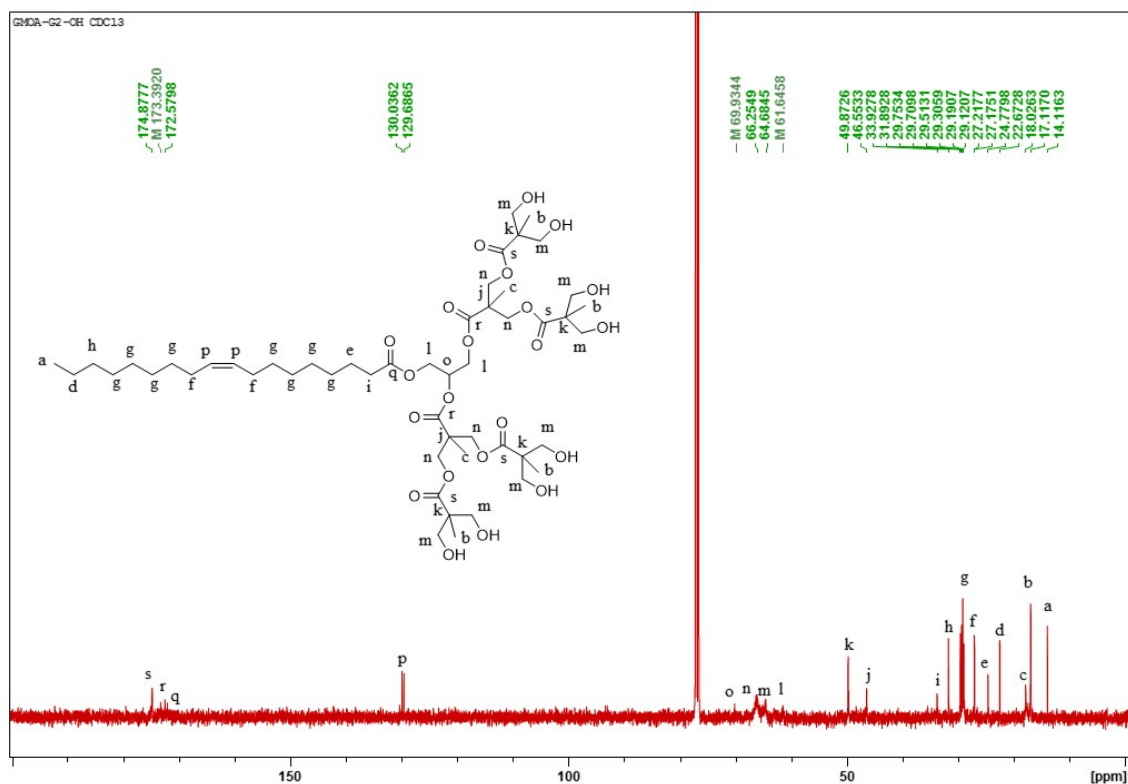


Fig. S50.  $^{13}\text{C}$  NMR of GMOA-G2-OH.

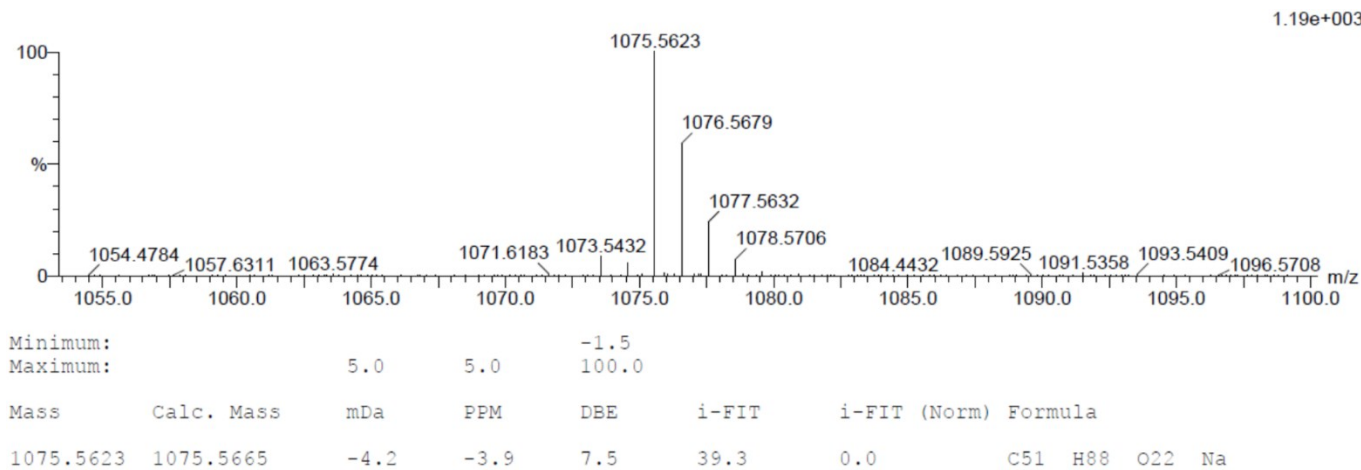


Fig. S51. HRMS of GMOA-G2-OH.



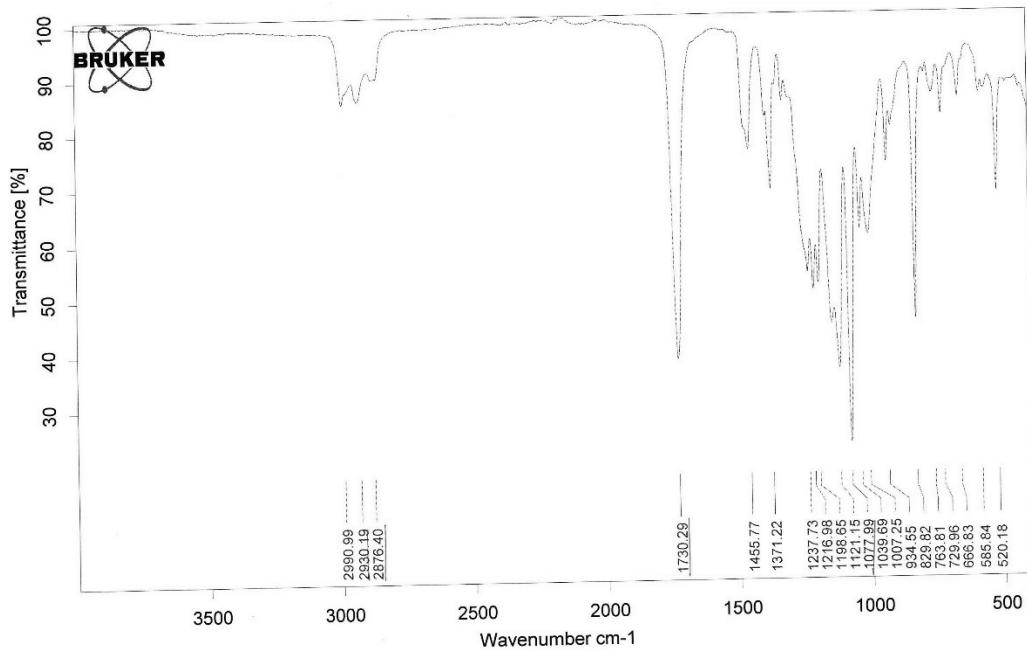


Fig. S52. FT-IR spectra of GMOA-G3-Me.

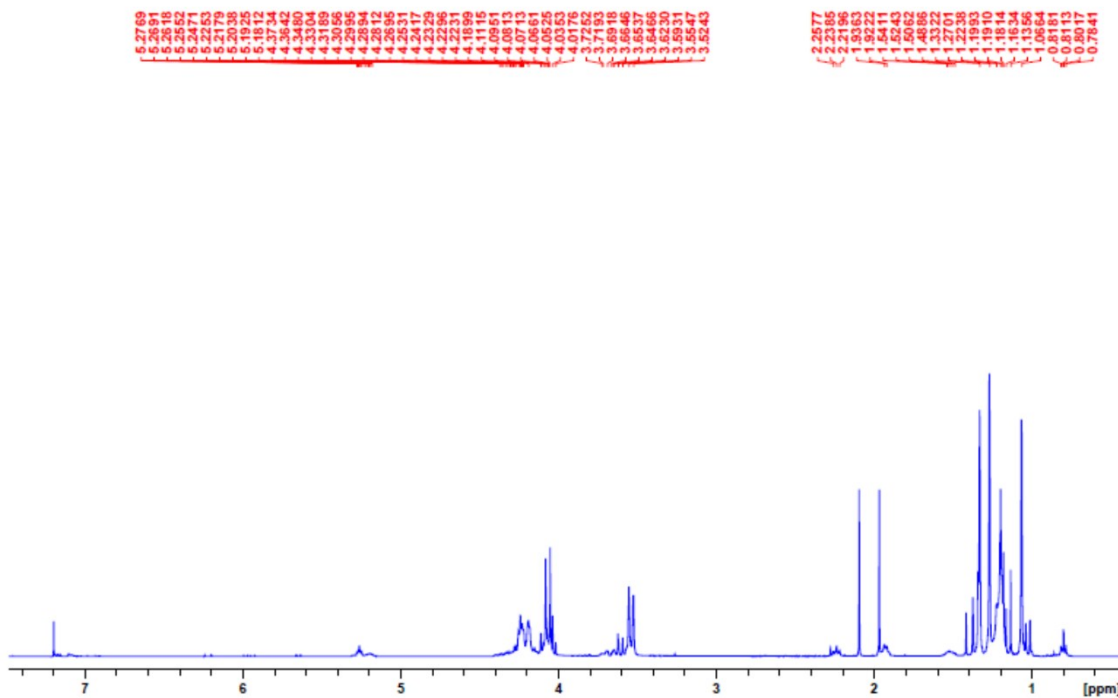


Fig. S53. <sup>1</sup>H NMR of GMOA-G3-Me.

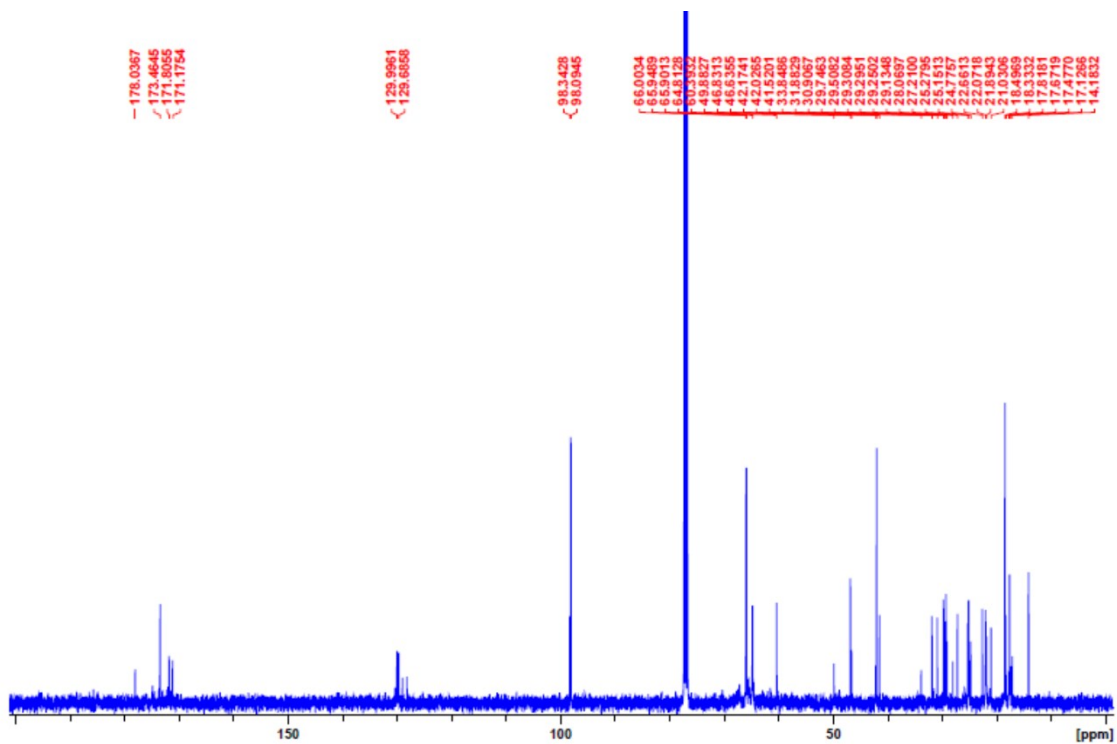


Fig. S54.  $^{13}\text{C}$  NMR of GMOA-G3-Me.

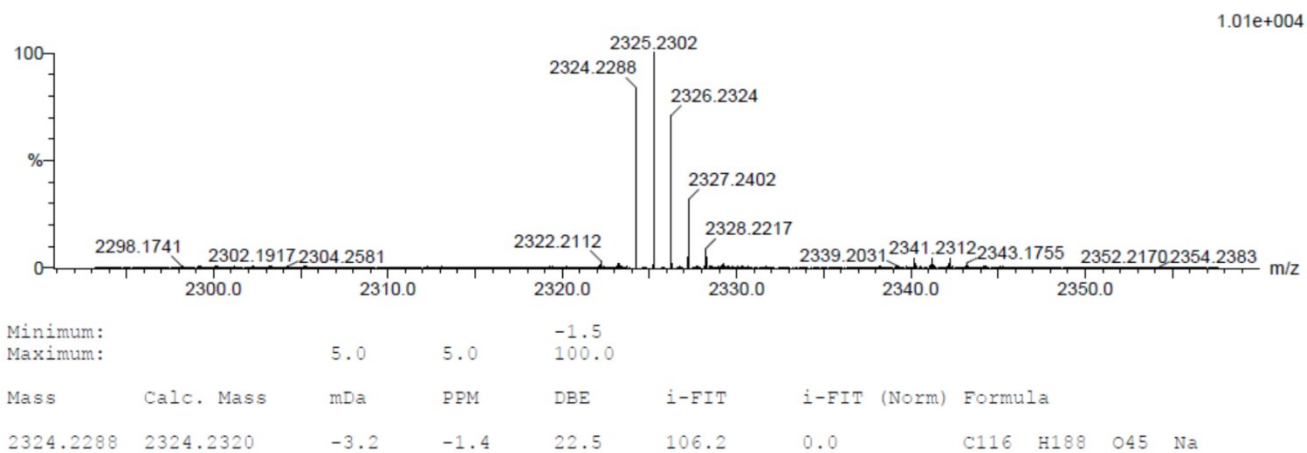


Fig. S55. HRMS of GMOA-G3-Me.

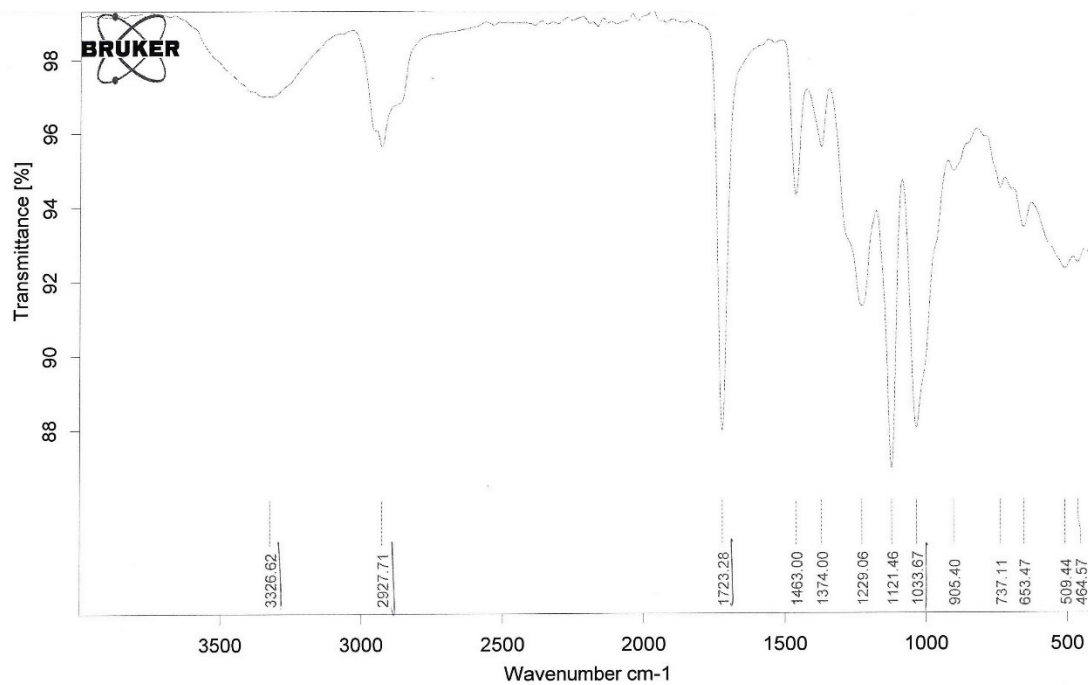


Fig. S56. FT-IR spectra of GMOA-G3-OH.

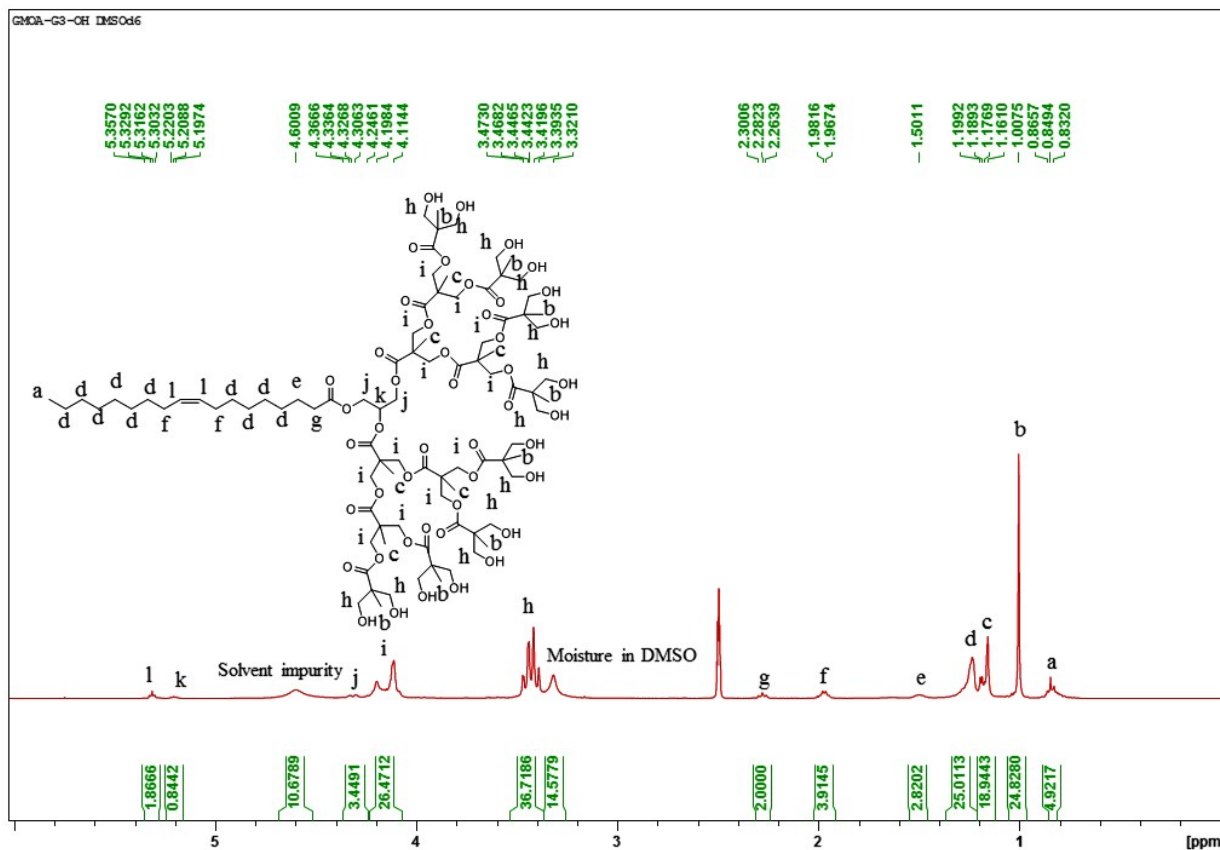


Fig. S57. <sup>1</sup>H NMR of GMOA-G3-OH.

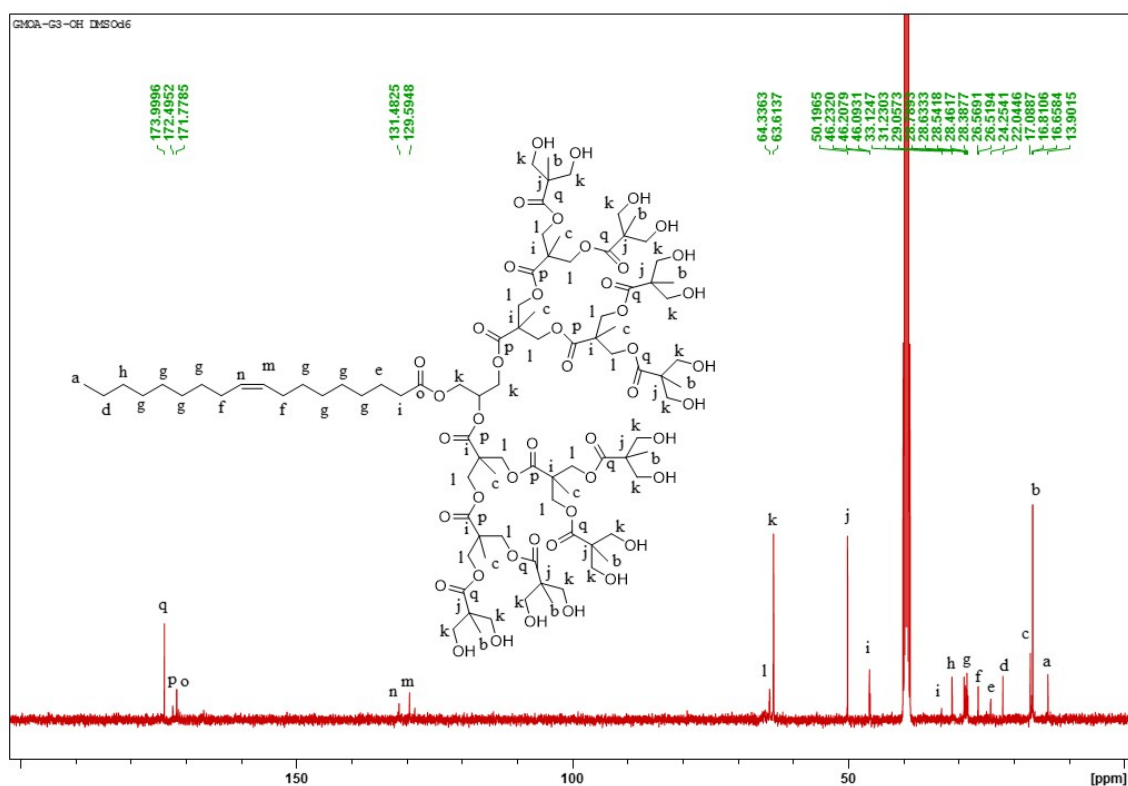


Fig. S58. <sup>13</sup>C NMR of GMOA-G3-OH.

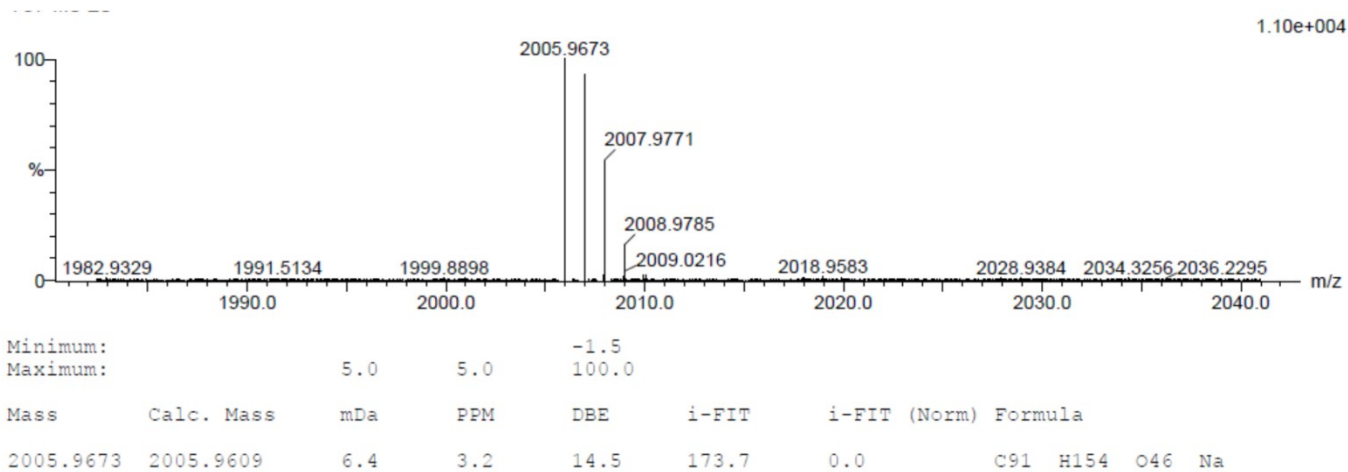


Fig. S59. HRMS of GMOA-G3-OH.

## References

1. Surfactant micelle characterization using dynamic light scattering  
<http://www.malvern.com/en/pdf/secure/AN101104SurfactantMicelleCharacterization.pdf>,  
(accessed 23 January 2016).
2. A. H. Hikal, A. Shibl and S. El-Hoofy, *Journal of Pharmaceutical Sciences*, 1982, **71**, 1297-1298.
3. L.-L. Cai, P. Liu, X. Li, X. Huang, Y.-Q. Ye, F.-Y. Chen, H. Yuan, F.-Q. Hu and Y.-Z. Du, *International Journal of Nanomedicine*, 2011, **6**, 3499-3508.